Fibrous hydrogels by electrospinning: Novel platforms for biomedical applications

Ji Woo Lee[1] and Kwang Hoon Song[1,2] (iD)

Abstract

Hydrogels, hydrophilic and biocompatible polymeric networks, have been used for numerous biomedical applications because they have exhibited abilities to mimic features of extracellular matrix (ECM). In particular, the hydrogels engineered with electrospinning techniques have shown great performances in biomedical applications. Electrospinning techniques are to generate polymeric micro/nanofibers that can mimic geometries of natural ECM by drawing micro/nanofibers from polymer precursors with electrical forces, followed by structural stabilization of them. By exploiting the electrospinning techniques, the fibrous hydrogels have been fabricated and utilized as 2D/3D cell culture platforms, implantable scaffolds, and wound dressings. In addition, some hydrogels that respond to external stimuli have been used to develop biosensors. For comprehensive understanding, this review covers electrospinning processes, hydrogel precursors used for electrospinning, characteristics of fibrous hydrogels and specific biomedical applications of electrospun fibrous hydrogels and highlight their potential to promote use in biomedical applications.

Biomedical applications of fibrous hydrogels fabricated via electrospinning techniques

There have been efforts to mimic characteristics of extracellular matrix (ECM), three-dimensional (3D) fibrous networks that involve diverse biomolecules and play important roles in various cell behaviors and responses,[1–3] with biomaterials for biomedical applications, and one way to mimic ECM is using hydrogels that are hydrophilic polymer networks and amendable through chemical modifications.[3,4] For instance, appropriate mechanical properties (stiffness and elasticity) of hydrogels, which might be similar to target tissue, could be determined by variation of hydrogel composition and density.[5–7] Additionally, hydrogels could be degraded by cells and adhesive to cells via introducing degradable crosslinkers and adhesive ligands, respectively, to hydrogels.[5,8–10] Geometry of ECM, nanofiber complex, has been also

regarded as an important feature influencing directional cell migration,[11] cell spreading,[12] and proliferation.[13] Diverse biofabrication techniques such as electrospinning,[14,15] solution blowing,[16,17] self-assembly,[18,19] and drawing[20,21] have been developed to fabricate various polymers including hydrogels in fibrous form to mimic ECM structures. Advantages and disadvantages of these techniques used for fabrication of fibrous hydrogels are shown in Table 1. In particular, electrospinning techniques

[1]Department of Nano-Bioengineering, Incheon National University, Incheon, Republic of Korea
[2]Research Center of Brain-Machine Interface, Incheon National University, Incheon, Republic of Korea

Corresponding author:
Kwang Hoon Song, Department of Nano-Bioengineering, Research Center of Brain-Machine Interface, Incheon National University, 119 Academy-ro, Yeonsu-gu, Incheon 22012, Republic of Korea.
Email: khsong@inu.ac.kr

Table 1. Advantages and disadvantages of techniques for fabrication of fibrous hydrogels.

Techniques for fibrous hydrogels	Advantage	Disadvantage	Ref.
Electrospinning	Simple process Inexpensive equipments Versatile and continuous fibers	Requirement of high voltage Difficulty to obtain 3D structure	Silva et al.[25] and Elnabawy et al.[26]
Solution blowing	High productivity Available with wide range of materials	Difficulty to obtain 3D structure Non-uniform fiber morphology Requirement of high pressure	Elnabawy et al.,[26] Gao et al.[27] and Zheng and Wang.[28]
Self-assembly	No requirement of equipment Large-scale production	Limited to specific materials Complex process Low productivity	Tan et al.[29] and Zagorodko et al.[30]
Drawing	Production of long fibers Large-scale production	Limited to specific materials Complex process	Shen et al.[31]

and its variants (co-axial electrospinning,[22] wet electrospinning,[23] and needleless electrospinning[24]) were utilized to generate diverse types of fibrous hydrogels.

Electrospinning is a technique to produce polymeric micro/nanofibers and have been used to generate fibers with various polymers for diverse applications. Typically, diameters of electrospun fibers, controlled by electrospinning setup (voltage applied to a needle, flow rate of precursors, and distance between a needle and a collector)[32–35] and viscosity of precursors,[36] vary from some $10\,nm$ to $10\,\mu m$,[37] and various approaches (rotating collector, gap electrospinning, and magnetic field-assisted electrospinning) were developed to manipulate alignment of fibers.[38–41] These micro/nanofibers were electrospun with various materials such as poly (ε-caprolactone) (PCL),[42–44] polylactic acid (PLA),[45,46] poly (D, L-lactic-co-glycolic) acid (PLGA),[47–50] polyurethane (PU),[51–53] and polyacrylonitrile (PAN)[54,55] and used for drug delivery, wound dressings, and vascular graft applications.

In particular, electrospun micro/nanofibers fabricated with hydrogels (methacrylated dextran (DexMA), gelatin methacryloyl (GelMA), and poly (vinyl-alcohol) (PVA)) have been used for various biomedical applications because they had potential to mimic ECM and their characteristics could be expanded by variation of hydrogel types. For example, electrospun fibrous hydrogels soft enough for cells to deform were used to study cell behaviors and responses.[56–60] Fibrous hydrogels cells could adhere were developed as scaffolds and used to regenerate tissues.[61–67] Degradable fibrous hydrogels involved drugs and biomolecules and delivered them through degradation of micro/nanofibers after implantation.[61,64,65] In addition, electrospun fibrous hydrogels that could exhibit pH-sensitive volume expansion[68] or glucose-sensitive enzymatic activities[69] were used to develop biosensors.

To promote use of electrospun fibrous hydrogels for biomedical applications, this review focuses on fabrication of electrospun fibrous hydrogels and their biomedical applications. Specifically, general electrospinning setup, hydrogel precursor types, and hydrogel crosslinking methods were

included to provide information on fabrication methods and types of fibrous hydrogels already used for biomedical applications. Additionally, their biomedical applications such as cell culture platform used for cell-related studies, implantable scaffolds to regenerate tissue after implantation, wound dressings to recover wounded skins, and biosensors to sense pH or glucose levels (Figure 1) were described for further applications to biomedical fields.

Fabrication of electrospun fibrous hydrogels

Electrospinning techniques have been used to generate micro/nanofibers that were made of diverse polymers including hydrogels and exploited for numerous biomedical applications. In general, electrospinning setup is composed of a power supply to apply voltage to a metal needle, a collector grounded, and a syringe pump to constantly supply polymer precursors through the metal needle in a controlled flow rate (Figure 2(a)). At a constant pumping of polymer precursors with application of voltage to a needle, a droplet of polymer precursors, formed at a needle tip, is stretched out by electrostatic repulsion applied to the droplet and ejected as micro/nanofibers toward the grounded collector when the electrostatic repulsion overcomes surface tension of the droplet (Figure 2(b)).[70,71] Solvents of precursors evaporate during flight of the liquid jet, and solid fibers are finally collected on the collector. Additionally, there are modified electrospinning techniques to fabricate various fibrous hydrogels with hydrogel precursors (Figure 3). For instance, co-axial electrospinning technique was used to generate fibers with two different materials separated at the core and the sheath of the fibers. In wet electrospinning, grounded collector was immersed in a coagulation bath to fabricate fibrous hydrogel mats with relatively low fiber packing density. Needless electrospinning setup could generate multiple jets to increase productivity of hydrogel fibers. Advantages and disadvantages of these electrospinning techniques are described in Table 2. Typically, fibers in diameters of some
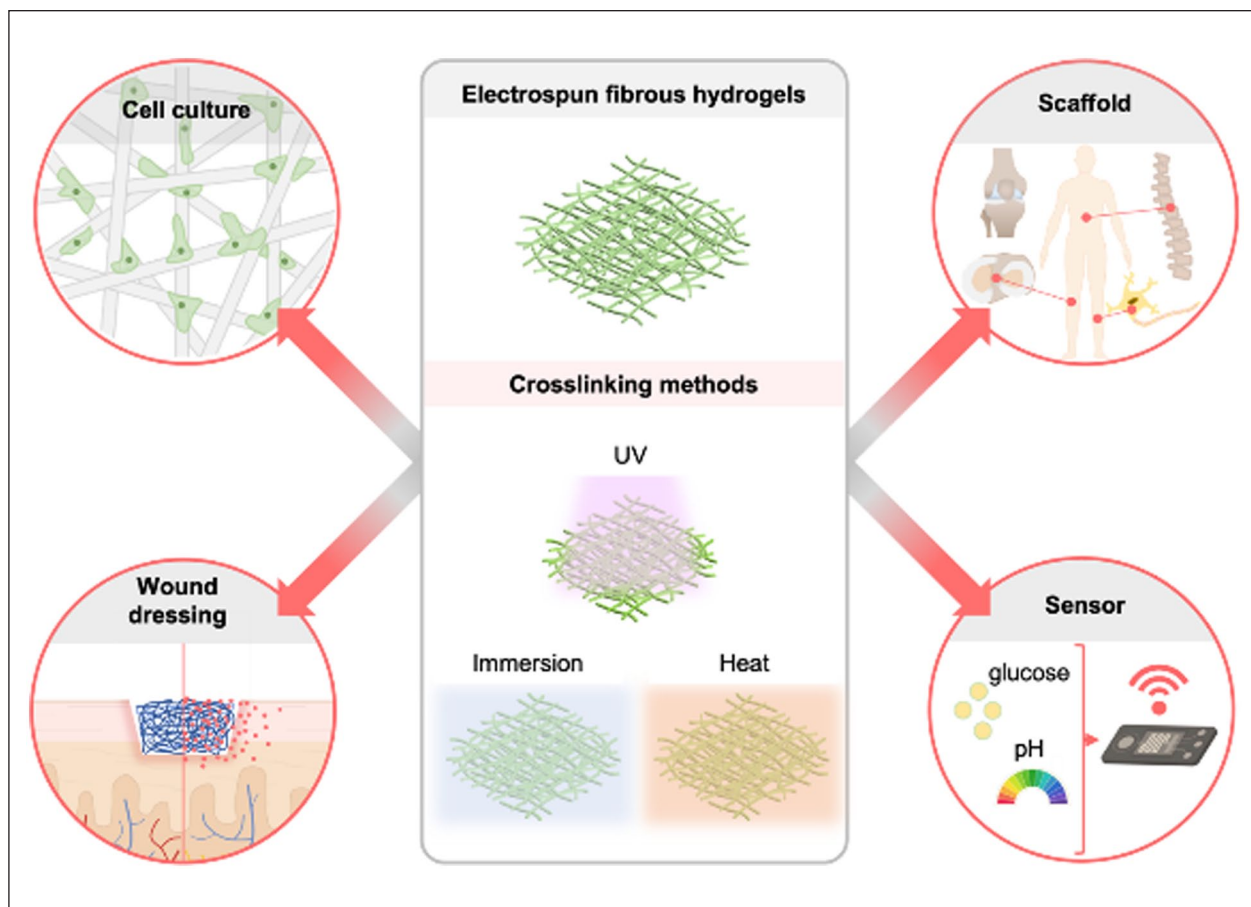
Figure 1. Crosslinking methods for fibrous structure stabilization and biomedical applications (cell culture platforms, implantable scaffolds, wound dressings, and biosensors) of electrospun fibrous hydrogels.
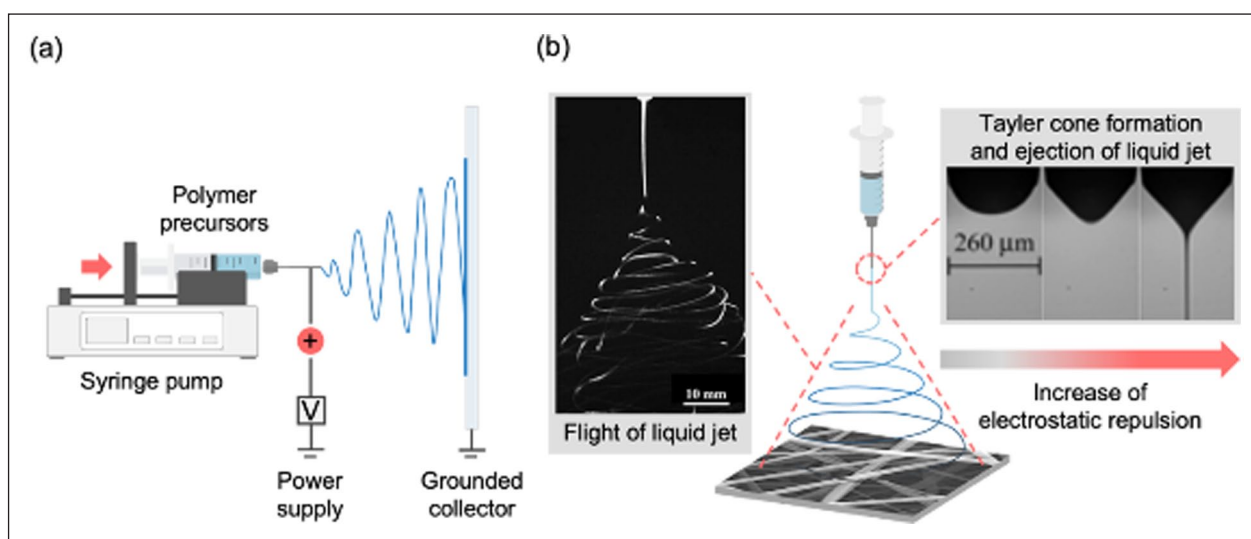

Figure 2. A schematic illustration of general electrospinning setup and processes. (a) General electrospinning setup. It is mainly composed of a syringe pump ejecting hydrogel precursors in a controlled flow rate, a power supply to apply voltage to a metal needle and a collector to collect polymeric fibers. (b) Overall processes to generate electrospun fibers. A droplet of polymer precursor at a needle tip is ejected toward a grounded collector when electrostatic repulsion exceeds surface tension of the droplet. Reproduced from Han et al.,[79] Chen et al.,[65] and Marginean et al.[80]
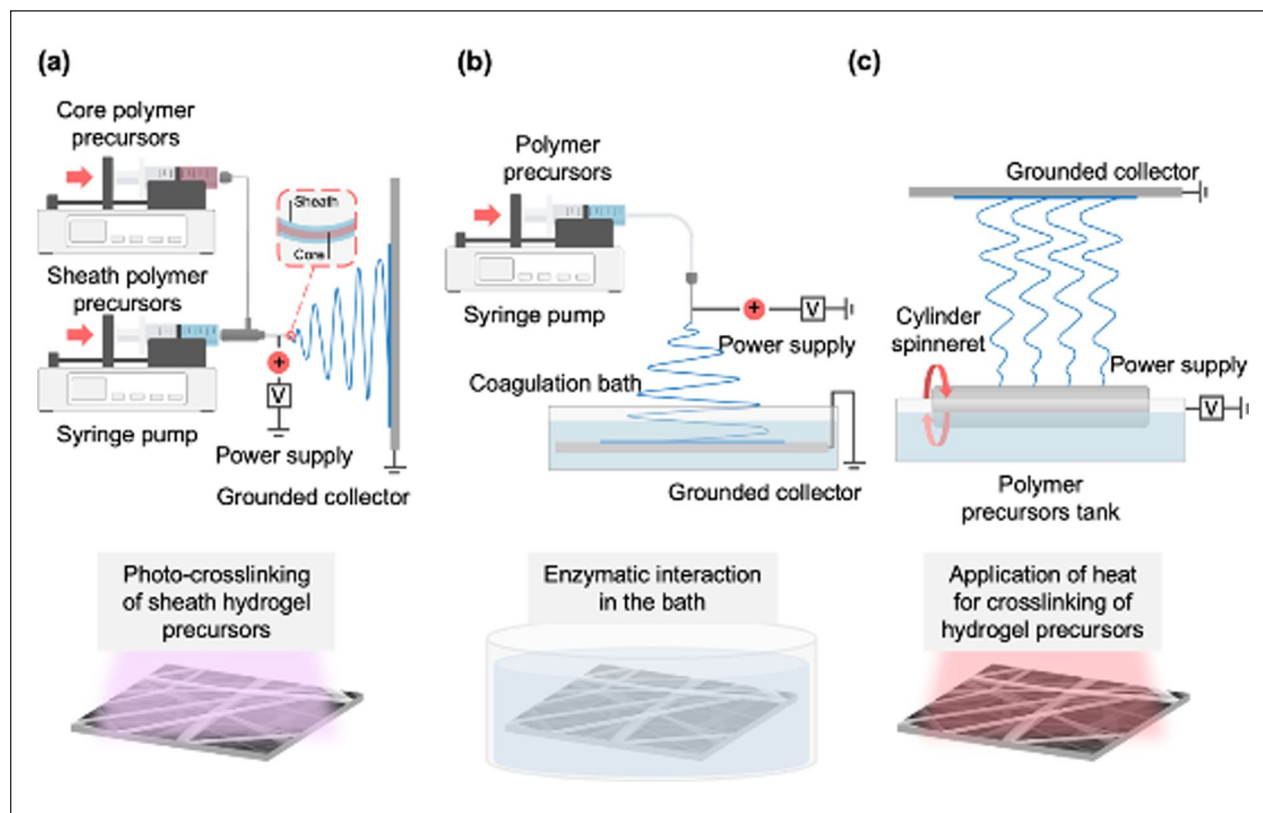
Figure 3. Various types of electrospinning techniques with crosslinking steps used for fabrication of electrospun hydrogel fibers. A power supply and a grounded collector are commonly required for electrospinning techniques: (a) co-axial electrospinning technique uses a co-axial needle to obtain fibers composed of one material at the core and another one at the sheath, (b) wet electrospinning technique uses a coagulation bath containing a grounded collector to fabricate fibrous hydrogel mats with relatively low fiber packing density, and (c) needleless electrospinning technique generates multiple jets to increase productivity of fibrous hydrogels. Reproduced from Chen et al.[65]

Table 2. Advantages and disadvantages of the electrospinning techniques used for fabrication of fibrous hydrogels.

Electrospinning techniques	Advantage	Disadvantage	Ref.
Co-axial electrospinning	Multi-functional properties from a single fiber	Limited combination of materials	Li et al.[22] and Han and Steckl.[81]
Wet electrospinning	Relatively increased inner porosity	Limited to water-insoluble materials	Majidi et al.[23] and Xu et al.[82]
Needleless electrospinning	High productivity	Necessity of using relatively higher voltage Inconsistent fiber morphology	Cengiz-Çallioğlu[24] and Partheniadis et al.[83]

hundred nanometers were obtained, and the diameter can be controlled by manipulating voltage, distance from a needle to a collector, and flow rate and viscosity of polymer precursors.[36,72,73] Additionally, thickness[74,75] and porosity[76,77] of fibrous mat and alignment[78] of fibers can be controlled by various approaches.

In general, hydrogel precursors loaded into syringes are electrospun to collect dried micro/nanofibers, and crosslinking steps are followed for stabilization of fibrous structures. For biomedical applications, diverse types of hydrogel precursors have been used to generate fibrous hydrogels

with various characteristics (Table 3). Specifically, photo-crosslinkable hydrogel precursors such as precursors containing MeHA,[58] NorHA,[60] HEMA-HA,[61] GelMA,[63,64] or γ-PGA-Nor/γ-PGA-SH[66] with photoinitiators and with/without crosslinkers have been exploited for fabrication of fibrous hydrogels. As photoinitiator, Irgacure 2959 has been widely used.[84] Other than that, POH/POA precursors and PVA/CS precursors were crosslinked through in situ crosslinking.[59,65] Gel-HPA[57] and fibrinogen[62] precursors were crosslinked through enzymatic reaction by HRP with H_2O_2 and thrombin, respectively. Gelatin/PLGA precursor

Table 3. Composition of hydrogel precursors used for electrospinning, crosslinking methods for the electrospun micro/nanofibers, diameter of fibers, and their biomedical application.

Precursors (Polymer)	Solvent	Others	Crosslinking Methods	Diameter of fibers	Biomedical application	Ref.
Gel-HPA	1:9 mixture of Milli-Q water and HFIP	-	Immersion in ethanol-water solution where the HRP was 10 unit/mL and H_2O_2 was 100 mM for 24 h	1.2 μm	Cell culture platform for HUVECs	Nie et al.[57]
MeHA + PEO	DI water	0.05% Irgacure 2959	Exposure of UV light under nitrogen (15 mW/cm² for 20 min)	1.95 μm (soft) 1.97 μm (stiff)	Cell culture platform for primary hepatic stellate cells	Davidson et al.[58]
POH + PEO/POA + PEO	DMEM	Cells (added to the POH + PEO precursor)	In situ crosslinking (electrospinning precursors containing hydrazide and aldehyde groups using a double barrel syringe)	2.2 μm	Cell culture platform for 3T3 cells	Xu et al.[59]
NorHA + PEO	DI water	DTT, 0.05% Irgacure 2959	Exposure of UV light (10 mW/cm² for 1 h on each side of fiber mat)	700 nm	Cell culture platform for hMSCs	Davidson et al.[60]
HEMA-HA + PEO	DI water	0.05% Irgacure 2959, 50 μg/mL PDGF-AB	Exposure of UV light under nitrogen (10 mW/cm² for 15 min on each side of fiber mat)	308 nm	Scaffold for dense connective tissue regeneration	Qu et al.[61]
Gelatin + PLGA	HFIP	5 mL of HA + PEO in DI water mixed with 5 g of fragmented fibers for fiber inks	Immersion in EDC/NHS (5%/3%) in 95% ethanol for 12 h, followed by immersion in water for 24 h	-	Scaffold for cartilage regeneration	Chen et al.[67]
Fibrinogen + PEO	Saline	-	Using rotating collector (50 rpm) in a bath containing 100 mM $CaCl_2$, and 10 units/mL thrombin solution	100 nm	Scaffold for peripheral nerve regeneration	Du et al.[62]
GelMA	HFIP	-	Immersion in 0.5 g Irgacure 2959 in 10 mL anhydrous alcohol, followed by exposure of UV light (for 60 min)	1 μm	Scaffold for spinal cord regeneration	Chen et al.[63]
GelMA	1:1 mixture of DI water and ethanol	-	Immersion in 3 wt% Irgacure 2959 in ethanol, followed by exposure of UV light (for 15 min)	350 nm	Wound dressing	Zhang et al.[64]
PVA + CS	Distilled water (for PVA), 1 wt% of acetic acid (for CS) (the mixture of PVA-CS in 6:4 weight ratio)	1 wt% DFO (added to the CS precursor)	Blend in-situ crosslinking reaction by mixing PVA and CS in an acid solution (the strong intermolecular hydrogen bonds)	716.5 nm	Diabetic wound dressing	Chen et al.[65]
γ-PGA-Nor + γ-PGA-SH + PEO	Water	1 wt% GS-Rg3 in methanol (the mixture of precursor and drug solution at 4:1)	Immersion in 0.05 wt% Irgacure 2959 in methanol, followed by exposure of UV light (5 mW/cm² for 45 min)	1.31 μm	Wound dressing for preventing hypertrophic scars	Xu et al.[66]
PVA + PAA	Milli-Q water	-	Heat treatment (145°C for 30 min)	330 nm	pH-sensitive biosensor	Shaibani et al.[68]
PVA + β-CD	Distilled water (for PVA), PBS (for β-CD) (the mixture of PVA-β-CD at 3:1)	0.4 g GOx in the β-CD precursor, 3 mL AuNPs in the PVA precursor, 0.2 g BTCA in PVA + β-CD precursor	Heat treatment (110°C for 6 h)	315 nm	Glucose-sensitive biosensor	Kim and Kim.[69]

Gel-HPA: gelatin-hydroxyphenylpropionic acid; HFIP: hexafluoroisopropanol; HRP: horseradish peroxidase; HUVECs: human umbilical vein endothelial cells; MeHA: methacrylated hyaluronic acid; PEO: poly(ethylene oxide); DI water: deionized water; Irgacure 2959: 2-hydroxy-4′-(2-hydroxyethoxy)-2-methylpropiophenone; UV: ultraviolet; POH: hydrazide-functionalized poly(oligoethylene glycol methacrylate); POA: aldehyde-functionalized poly(oligoethylene glycol methacrylate); DMEM: Dulbecco's Modified Eagle's Medium; NorHA: norbornene-modified hyaluronic acid; DTT: dithiothreitol; hMSCs: human mesenchymal stem cells; HEMA-HA: hydroxyethyl methacrylate modified hyaluronic acid; PDGF-AB: platelet-derived growth factor-AB; EDC: (N-ethyl-N′-(3-(dimethylamino)propyl)carbodiimide); NHS: N-hydroxysuccinimide; CS: chitosan; DFO: desferrioxamine; γ-PGA-Nor: norbornene-modified poly(γ-glutamic acid); GS-Rg3: ginsenoside Rg3; PAA: poly(acrylic acid); β-CD: β-cyclodextrin; PBS: phosphate-buffered saline; GOx: glucose oxidase; AuNPs: gold nanoparticles; BTCA: 1,2,3,4-butanetetracarboxylic acid.

Figure 4. Comparison between characteristic of bulk hydrogel and fibrous hydrogel. Bulk hydrogels were referred to hydrogels in millimeter to centimeter scales, and diameters of electrospun fibrous hydrogels were generally in nano/micrometer scales. Fabrication methods could determine overall shapes of bulk and fibrous hydrogels. Physical properties (Stiffness, porosity, alignment and deformability) of fibrous hydrogels might induce cellular behaviors different from cellular behaviors influenced by those properties of bulk hydrogels.

was crosslinked through coupling reaction of EDC/NHS.[67] Lastly, PVA/PAA and PVA/β-CD precursors were crosslinked through heat treatment.[68,69] Additionally, viscoelasticity is an important property of the precursors to generate electrospun micro/nanofibers, and PEO, water-soluble and biocompatible polymer, are often added to the precursors to meet viscoelasticity proper to implement electrospinning.

Characteristics of electrospun fibrous hydrogels

Fibrous hydrogels fabricated with various electrospining techniques exhibit distinct characteristics compared to those of bulk hydrogels, due to the difference in scale and structure of those hydrogels (Figure 4). In general, diameters of fibrous hydrogels obtained through electrospinning techniques were in micro/nanoscales while hydrogels in millimeter to centimeter scales were defined as bulk hydrogels.[85] Overall structures of bulk and fibrous hydrogels can be determined by various fabrication techniques. 3D printing,[86,87] lithography,[88] and molding[89,90] techniques allowed fabrication of bulk hydrogels in user-defined and complex structures. Likewise, double layers of fibrous hydrogels were obtained by electrospinning two different materials successively,[59,91] and bundles[62,63] and a hollow conduit[92] were prepared by rolling electrospun fibrous hydrogel mats. Additionally, fibrous hydrogels in user-defined 3D structures were formed by 3D printing of jammed fragmented fibrous hydrogels.[60]

Physical properties of bulk and fibrous hydrogels, such as stiffness, porosity, alignment, and deformability, can possibly affect various cellular behaviors in different manners. For instance, elevation of fibrous hydrogel stiffness decreased cellular proliferation and spreading while elevation of bulk hydrogel stiffness increased the proliferation and spreading.[56,58] Similarly, porosity and alignment of fibrous hydrogels, different from those of bulk hydrogels in scale and structure, might induce cellular behaviors that are different from cellular behaviors influenced by pores and aligned structures of bulk hydrogels. Due to the different scale and structure of bulk and fibrous hydrogels, deformability of those hydrogels was also different to each other. Through the cellular contraction, a bulk hydrogel in a cylindrical shape shrank and a hydrogel membrane was rolled.[93–95] On the other hand, cells on and within fibrous hydrogels significantly deformed adjacent fibrous hydrogels irregularly[56,60] although overall structures of fibrous hydrogels might be also deformed like bulk hydrogels (It was shown that cells within fibrous hydrogels changed overall fibrous hydrogel shapes via contraction[60]). These all imply that cellular behaviors on and within fibrous hydrogels can be different from cellular behaviors on and within bulk hydrogels. Specifically, 3T3 fibroblast cells cultured within fibrous POA + POH hydrogels showed higher viability than cells cultured in flat bulk hydrogels (Figure 5(a)).[59] Differentiation of myofibroblasts in bulk dextran vinyl sulfone (DexVS) hydrogels was decreased with elevation of hydrogel stiffness while fibroblasts in the hydrogels containing fibrous hydrogels were primed for activation into myofibroblasts via interaction with fibrous hydrogels (Figure 5(b)).[15] Additionally, human pulmonary artery smooth muscle cells (hPASMCs) on fibrous hydrogels infiltrated deeper than cells on bulk hydrogel platforms (Figure 5(c)).[96] Possibly, fibrous hydrogels can
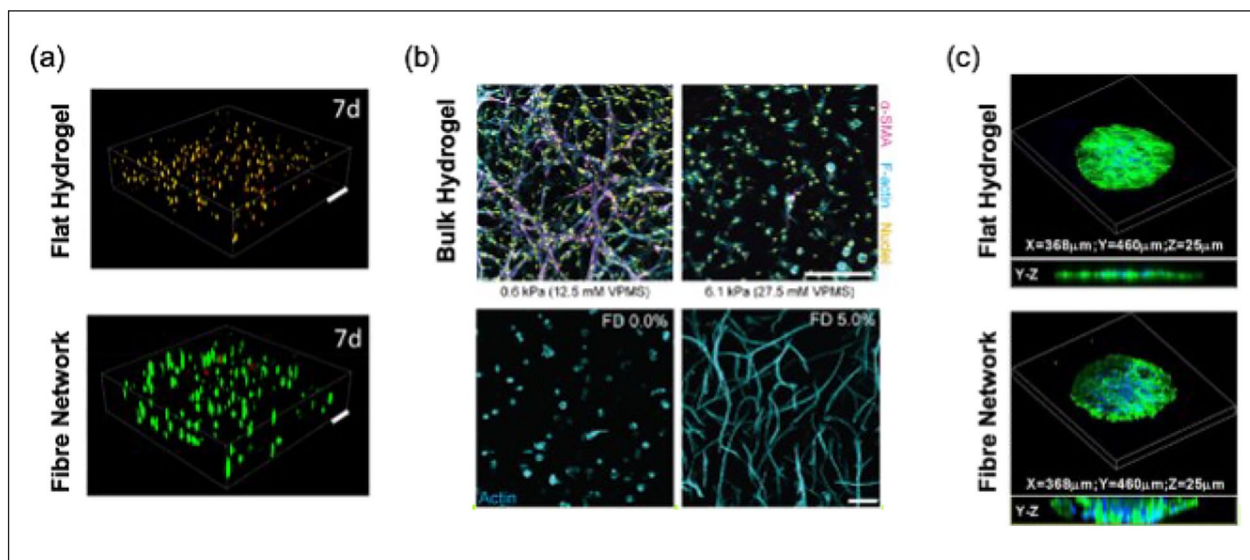
Figure 5. Comparisons of cellular behaviors on/within bulk and fibrous hydrogels. (a) Live/dead staining after 7 days of 3T3 cell culture in bulk hydrogels (top) and within fibrous hydrogels (bottom) (Scale bar: 200 μm). Reproduced from Xu et al.[59] Myofibroblast differentiation study in soft/stiff bulk hydrogels (top, scale bar:200 μm) and in hydrogels with 0.0% and 5.0% fiber density (bottom, FD: fiber density, scale bar: 100 μm). Stiffness of hydrogels was controlled by controlling concentration of crosslinkers (GCVPMS↓MRGGCG, VPMS). Reproduced from Matera et al.[15] Distributed under the Creative Commons Attribution NonCommercial License 4.0 (CC BY-NC, https://creativecommons.org/licenses/by-nc/4.0/). (c) Infiltration thickness of hPASMCs on bulk (left) and fibrous (right) hydrogels after 1 day of seeding. Reproduced from Ding et al.[96]
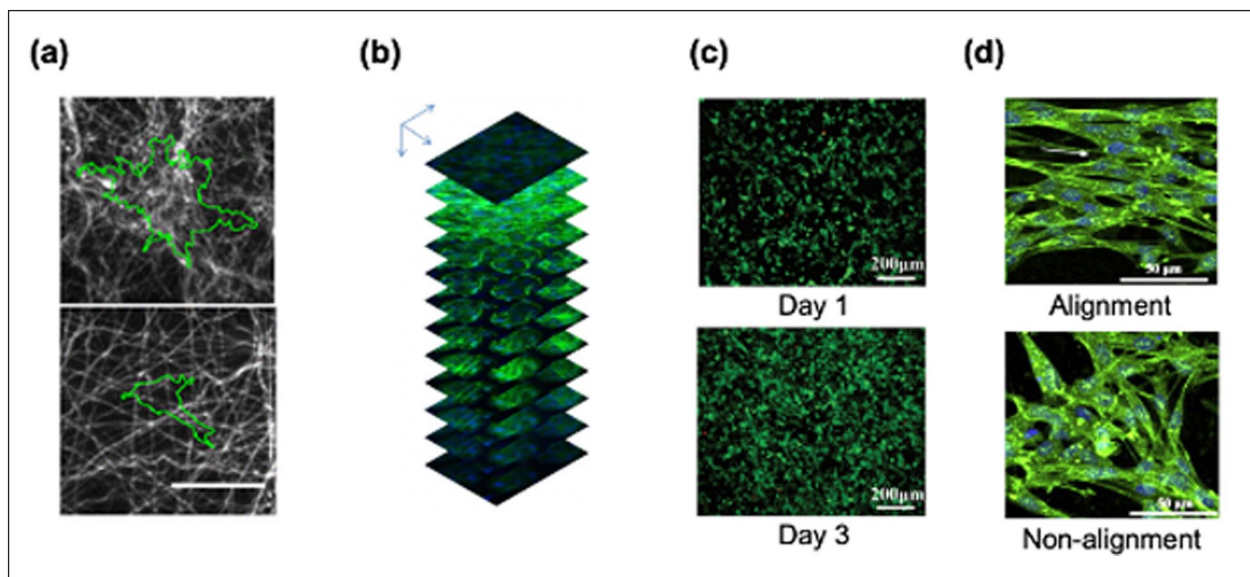

Figure 6. Cells on and within electrospun fibrous hydrogels were observed to investigate various cellular behaviors and responses. (a) Cell spreading on soft (top) and stiff (bottom) fibrous hydrogels after 7 days of cell culture. Reproduced from Davidson et al.[58] (b) Cell infiltration through fibrous hydrogels after 3 days of cell culture. Reproduced form Wang et al.[97] (c) Viability of cells on fibrous hydrogel membranes. Reproduced from Sun et al.[98] (d) Cells on aligned fibrous hydrogels (top) and randomly oriented ones (bottom) after 1 day of cell culture. Reproduced from Du et al.[62]

be useful in biomedical applications because relatively high cell viability and infiltration are expected from fibrous hydrogels. The fibrous hydrogels exhibiting distinct features were used to study various cellular behaviors although a few systemic comparisons between cell behaviors with bulk and fibrous hydrogels were implemented. Specifically, spreading (Figure 6(a)),[56,58] infiltration (Figure 6(b))[46,97] cell viability (Figure 6(c))[57,59,98] and alignment (Figure 6(d))[62,63] were studied with fibrous hydrogel environments.
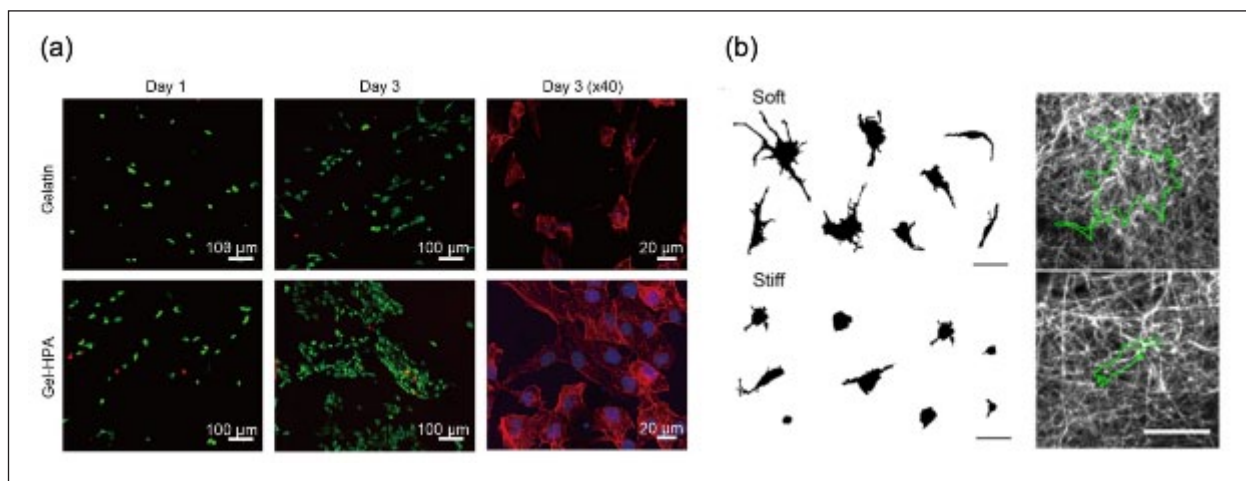
Figure 7. 2D cell cultures on electrospun fibrous hydrogels. (a) Live/dead staining (left, middle) and F-actin staining (right) of human umbilical vein endothelial cells (HUVECs) cultured on fibrous gelatin and Gel-HPA hydrogels on Day 1 and 3. Fibrous gelatin hydrogel was stiffer than fibrous Gel-HPA hydrogels. Reproduced from Nie et al.[57] Distributed under the Creative Commons Attribution 4.0 International License (CCBY 4.0, http://creativecommons.org/licenses/by/4.0/). (b) Activated stellate cells on soft/ stiff MeHA hydrogel nanofibers. Representative masks of cell outlines on soft/stiff nanofibers (left, scale bar: 50 μm) and fluorescent images of soft/stiff nanofibers under the cells (right, scale bar: 50 μm). Reproduced from Davidson et al.[58]

Taken together, electrospun fibrous hydrogels exhibit distinct characteristics compared to those of bulk hydrogels and were used for investigation of cellular behaviors.

Biomedical applications

In vitro cell culture platforms mimicking in vivo fibrous environments

2D platforms to study cellular behaviors. Diverse cell culture platforms have been developed and utilized for various applications. For example, traditional platform such as cell culture dishes providing wide and flat reservoirs to contain cells and cell culture media with relatively easy handling have been widely used although their mechanical properties and geometry that can possibly influence cell behaviors and fate are different from in vivo microenvironments. To meet needs of improvement in cell culture platforms, hydrogels to mimic ECM and microfabrication techniques to create in vivo-like microenvironments were applied to develop the platforms. Cells were grown on various hydrogels,[99–105] and cell differentiation and migration were studied by analyzing cells on hydrogels with stiffness alteration.[106,107] Microfluidic chips providing in vivo-like cell culture platforms were also used to study various cellular mechanisms[108–111] and even developed as organ-on-a-chip by mimicking features of specific organs.[112,113]

Alternatively, electrospun fibrous hydrogels sheets that have ECM-like topography and potential to mimic various ECM features have been used for 2D cell culture and cell behavior studies.[114,115] For instance, fibrous gelatin (relatively stiff) and Gel-HPA (relatively soft) hydrogel microfibers were fabricated by electrospinning and human umbilical vein endothelial cells (HUVECs) were cultured

on each hydrogel microfiber scaffold for 3 days (Figure 7(a)).[57] Higher cell viability and more cell spreading were observed on Gel-HPA fibers in comparison to the gelatin fibrous hydrogels, indicating that soft fibrous environments can enhance the cell adhesion and cell spreading.

Activated stellate cells were also cultured on soft and stiff MeHA hydrogel nanofibers functionalized with adhesive ligands, and their spreading area and phenotype were observed (Figure 7(b)).[58] The cells on soft nanofibers displayed larger spreading than cells on stiff nanofibers, and phenotype of the cells became quiescent on stiff nanofibers. In addition, soft and stiff DexMA hydrogel microfibers coupled with adhesive ligands were prepared via electrospinning of precursors and variation of crosslinking degree and used to study how geometry and stiffness of microfibers affect adhesion area and proliferation of human mesenchymal stem cells (hMSCs).[56] For comparison, spreading area and proliferation of those cells on type I collagen matrices with low and high concentration were also analyzed. On bulk hydrogels, spreading area and proliferation of hMSCs increased with an elevation of hydrogel stiffness. On the contrary, cell on fiber networks exhibited decreased spreading area and proliferation with a stiffness increase of fiber networks, similar to a trend observed from cell on collagen matrices.

These all imply that topography and stiffness of fibrous hydrogel sheets can greatly influence cells and need to be considered for cell cultures.

3D platforms to encapsulate cells within fibrous environments. Electrospun fibrous hydrogels in sheet forms have been used as 2D cell culture platforms in various studies because they were relatively easy to fabricate and handle. Those fibrous sheets were generally obtained by tightly
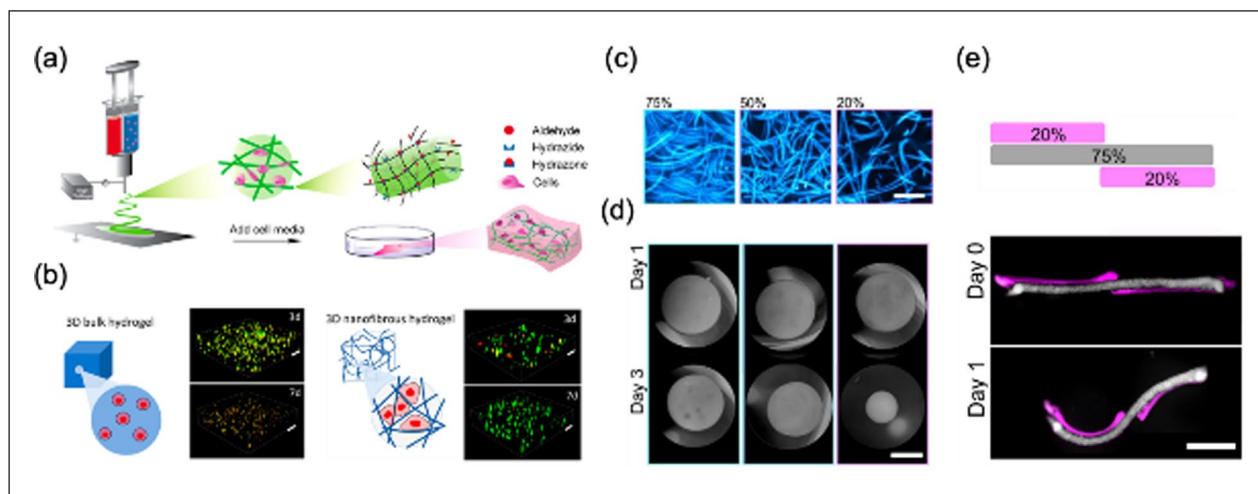
Figure 8. 3D cell culture within fibrous hydrogels. (a) A schematic illustration of processes to encapsulate 3T3 mouse fibroblast cells within fibrous hydrogels. (b) 3D confocal images of the cells encapsulated in bulk hydrogel (left) and electrospun hydrogel nanofibers (right) after 3 and 7 days of incubation (scale bar: 200 μm). Reproduced from Xu et al.[59] (c) Representative fluorescent images of NorHA nanofibers with varied nanofiber densities (75%, 50%, and 20%) (scale bar: 10 μm). (d) Representative inverted phase-contrast images of mesenchymal stem cells (MSCs) encapsulated within nanofibers on day 1 and 3 with varied nanofiber densities (75%, 50%, and 20%) (scale bar: 2 mm). (e) A schematic illustration (top) and representative images (bottom) of 3D-printed cell-laden nanofibers with 75% (gray) and 20% (pink) nanofiber densities (scale bar: 1 mm). Reproduced from Davidson et al.[60] Distributed under the Creative Commons Attribution NonCommercial License 4.0 (CCBY-NC, https://creativecommons.org/licenses/by-nc/4.0/).

stacking numerous electrospun fibers on collectors. The stacked micro/nanofibers often interfered cell migration through the fibrous sheets,[116] which could a huddle for them to be used as a 3D cell culture platform. In order to create fiber-based 3D microenvironments that can encapsulate cells for cell culture, strategies electrospinning precursors containing cells[59] and fabricating structures with fragmented nanofiber suspensions involving cells[60] were suggested.

To encapsulate 3T3 mouse fibroblast cells within electrospun hydrogel nanofibers, POH and PEO precursors including cells and POA and PEO precursors were electrospun together through a double barrel syringe with a relatively low voltage, 10 kV (Figure 8(a)).[59] Subsequently, electrospun nanofibers were stabilized via aldehyde and hydrazide interaction, and immediately transferred into cell culture media for cell culture. Viabilities of cells encapsulated in bulk hydrogel and fibrous hydrogel were also analyzed on day 3 and 7, and cells within fibrous environment exhibited higher viabilities than cells in bulk hydrogels (Figure 7(b)).

Alternatively, nanofiber suspensions were prepared by fragmenting electrospun NorHA nanofibers and suspending them with varied fiber density (Figure 8(c)),[60] and cells were encapsulated and cultured within nanofiber-based structures by forming and crosslinking nanofiber suspensions containing cells (Figure 8(d)). Interestingly, the overall structures containing MSCs with 20%, 50%, and 70% nanofiber densities contracted overtime through interaction between crosslinked nanofibers and the cells,

and degree of contraction increased with a decrease of nanofiber density. Exploiting the differences in contraction degree, curved membranes were also fabricated (Figure 8(e)). Specifically, the suspensions containing cells with 20% and 70% nanofiber densities were extruded within a support bath to form relatively flat and layered membranes, and the membranes were curved through the differences in contraction degree on day 1. This research demonstrated that 3D fibrous cell culture platforms could be fabricated with nanofiber suspensions and the suspensions had a potential to generate complex structures similar to tissues and organs.

Taken together, cells were cultured well within electrospun fibrous hydrogel-based 3D platforms, and further studies regarding cell behaviors within these platforms and development of platform in tissue-like structures are expected.

Scaffolds for tissue engineering

Implantable scaffolds for tissue regeneration. Electrospun hydrogel micro/nanofibers have been also applied to develop scaffolds that provide tissue-like structures to support tissue regenerations, exploiting their ECM-like geometries and abilities to mimic mechanical and chemical characteristics of local tissues.[61–63,117]

For example, HEMA-HA and PEO nanofibers together with PCL nanofibers were used to present strategies to regenerate knee meniscus (Figure 9(a)).[61] Specifically, the strategies included controlled release of biomolecules.
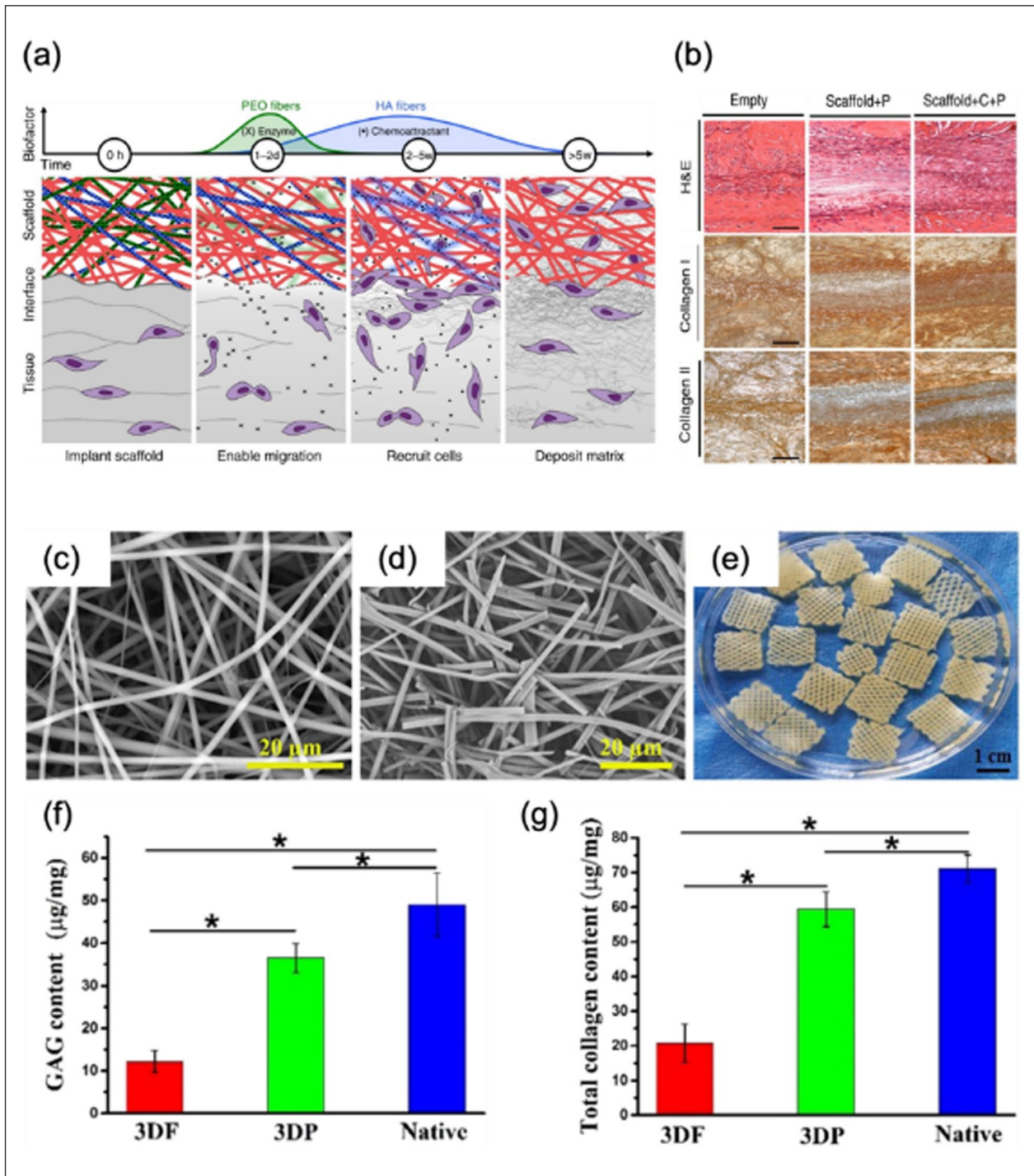
Figure 9. Implantable scaffolds developed with fibrous hydrogels for dense connective tissue regeneration. (a) A scheme of knee meniscus regeneration strategy using PEO and HA nanofibers releasing collagenase and PDGF-AB, respectively. (b) H&E staining and collagen type Ⅰ and Ⅱ immunostaining of the wounded meniscus tissues without scaffolds and with scaffolds containing PDGF-AB only and PDGF-AB with collagenase after 4 weeks of subcutaneous implantation (scale bar: 100 μm). Reproduced from Qu et al.[61] Distributed under the Creative Commons Attribution 4.0 International License (CCBY, http://creativecommons.org/licenses/by/4.0). (c) Electrospun gelatin/PLGA fibers and (d) the fragmented fibers. (e) Scaffolds 3D printed with gelatin/PLGA hydrogel fibers. Analysis of (f) GAG content and (g) total collagen content for evaluation of cartilage regeneration after 8 weeks of implantation. Reproduced from Chen et al.[67]

PEO nanofibers containing collagenase dissolved rapidly within tissue to improve cell migration through scaffolds by enlarging pores at scaffolds and implement burst delivery of collagenase, followed by a sustained delivery of PDGF-AB involved in HEMA-HA nanofibers. Rapid release of collagenase was to improve local cell migration via degrading tissue around implantation site, and relatively slow release of PDGF-AB was to recruit cells around the scaffolds. As a result, the scaffolds releasing collagenase and PDGF-AB improved cell migration through scaffolds, expecting rapid regeneration of meniscus tissues (Figure 9(b)).

Similarly, gelatin/PLGA fibers obtained by electrospinning (Figure 9(c))[67] were used to regenerate cartilages. Specifically, the fibers were fragmented by centrifuging fibers in tert-butanol (Figure 9(d)) and kneaded in HA and PEO solution to form 3D printable inks. Then, scaffolds were fabricated by molding with the inks and freeze-drying (3DF) and the other scaffolds with relatively large pores and high porosity were fabricated by 3D printing with the inks and freeze-drying (3DP). The scaffolds were implanted in cartilages of mice and evaluation of cartilage regeneration was implemented after 8 weeks. As a result, glycosaminoglycan (GAG) and total collagen content in the 3DP group were significantly higher than those in the 3DF group (Figure 9(f) and (g)). This result implied that cartilages in the 3DP group were regenerated more than those in 3DF group because of relatively high porosity and large pores in 3DP group.

Additionally, aligned fibrin hydrogel nanofibers (AFG) were developed as scaffolds to regenerate peripheral nerves (Figure 10(a)).[62] Larger gap at peripheral nerve often requires autograft to relay signals to avoid disorders in motor function and sensory perception. Instead of autograft, strategies using aligned nanofibers to guide axonal regeneration eventually for bridging the large gap were introduced in this research. AFG and randomly oriented fibrin hydrogel nanofibers (RFG) were implanted into 10 mm-nerve gaps at left femur of rats, and the AFG and autograft groups showed few hyperplastic collagen fibers in comparison to the RFG groups after 12 weeks of implantation (Figure 10(a)). Likewise, density, mean diameter of myelinated nerve fibers and thickness of myelin sheath were similar in both groups, implying that AFG could replace autograft in regeneration of peripheral nerves (Figure 10(b)).

Similarly, aligned GelMA microfibers obtained by electrospinning with customized parallel electrodes were developed as scaffolds to repair spinal cord (Figure 10(c)).[63] Promoted cell adhesion and guided directional growth were expected from microstructures of the scaffolds, and the scaffolds showed high cell viabilities. After 12 weeks of scaffold implantation to right hemisected spinal cord defect of rats, motor function recovery of hind limb was evaluated with the Basso, Beattie, and Bresnahan

(BBB) locomotor rating scale (Figure 10(d)). Compared to a control groups, the GelMA groups exhibited better recovery of motor functions.

Electrospun hydrogel micro/nanofibers were developed as implantable scaffolds, and tissues were regenerated by implanting those scaffolds. Considering characteristics and potential, these scaffolds can be further applied to regenerate other various tissues that have fibrous structures or require fibrous structures for efficient tissue regeneration.

Wound dressings to repair skin. Skins play important roles in sensory perception, homeostasis and protecting internal organs and tissues from infection and physical impact,[118] which can be interfered by severe skin wounds that might require large amount of time to recover. Thus, wound dressings with various recovery strategies including prevention of moisture loss and infection at wound sites have been developed to aid skin repair,[119–122] and electrospun hydrogel micro/nanofibers were also applied to fabricate wound dressings. Compared to conventional bulk hydrogel wound dressings, electrospun fibrous hydrogel wound dressing might provide larger surface area for cell adhesion and allow more cell infiltration through the dressing.

Electrospun GelMA nanofibers grafted with particles releasing drugs in response to increase of temperature were developed as wound dressings, and wound healing with these dressings was evaluated with full-thickness mouse skin defect models (Figure 11(a)).[64] On day 12 of wound healing assay with the skin defect models, wounds covered by GelMA nanofibers releasing drugs at body temperature (GelMA-polydopamine (PDA)-aspirin (ASP) group) showed more wound closure than wounds just recovered with cotton gauzes (Control group). Additionally, H&E staining on the day 12 allowed to verify that the skin repaired with the dressings showed high reepithelization and structure similar to normal skin (Figure 11(b)).

In addition, PVA/CS (PC) nanofibers loaded with PFO (PCD) expected to accelerate formation of blood vessels were used to treat full thickness of wounds on dorsum of diabetic rats (Figure 11(c)).[65] Promoted angiogenesis can be helpful for recovery of diabetic wound because formation of blood vessels delivering oxygen and nutrients required for wound healing can be inhibited by high level of glucose. As a result, wound closure was enhanced by using PC nanofibers releasing DFO. Increased expression of vascular endothelial growth factor (VEGF) and stromal cell-derived factor 1alpha (SDF-1α) was also verified when DFO was delivered to wound sites (Figure 11(d)).

γ-PGA-Nor/ γ-PGA-SH (PNS) microfibers involving GS-Rg3 and added with cell adhesion peptide (arginine-glycine-asparate-cysteine (RGDC)) (PNS-G-RGDC) were also used to treat wounds at back skin of rats (Figure 11(e)).[66] Gs-Rg3 that could suppress proinflammatory cytokines and downregulate VEGF expression was
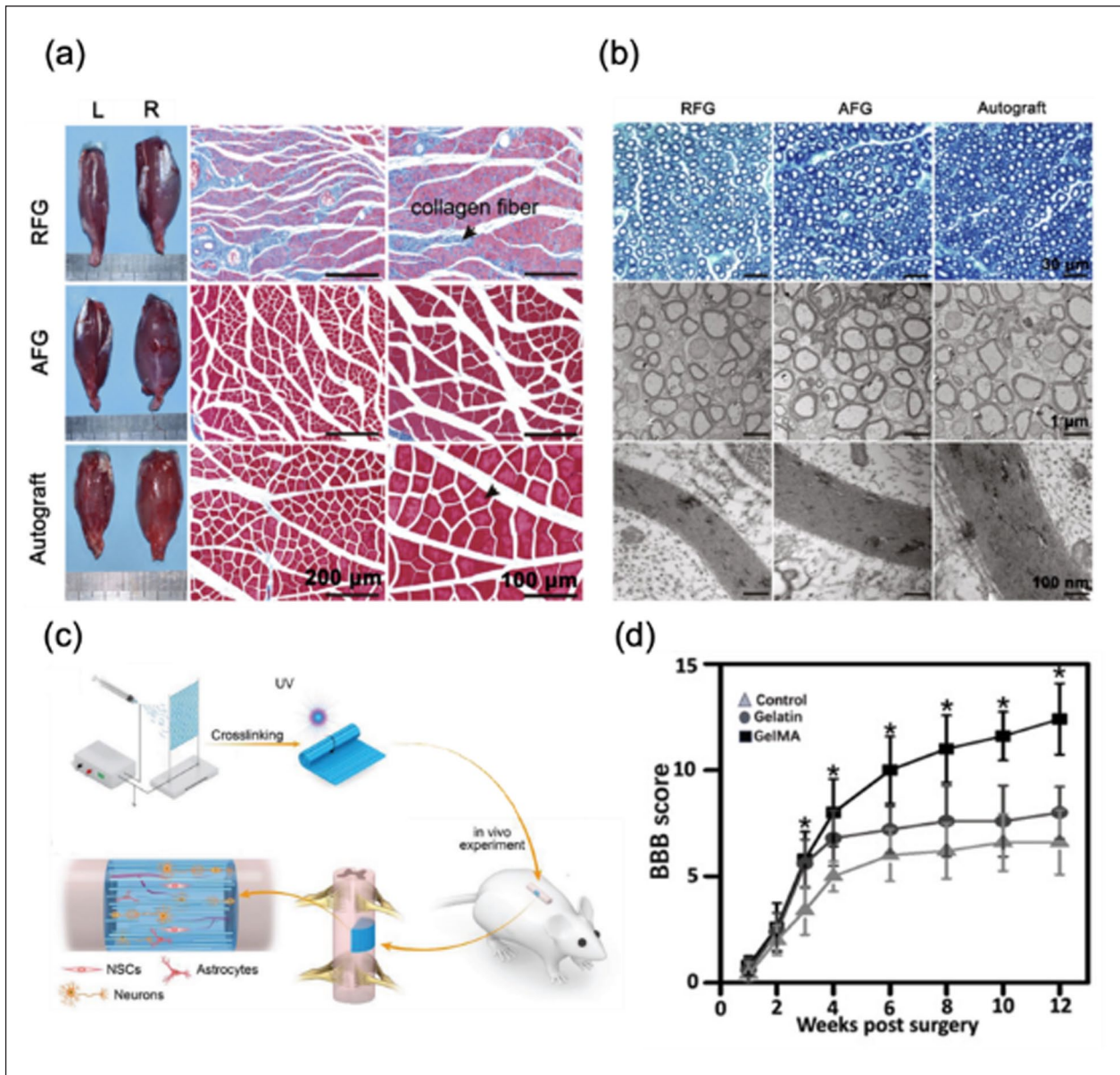
Figure 10. Implantable scaffolds developed with fibrous hydrogels to guide axonal regeneration. (a) Reinnervation of gastrocnemius at 12 weeks after implantation (left limb). Pictures of the isolated muscle and images of Masson's trichrome staining of the sectioned muscles from the injured limbs. RFG: randomly oriented fibrin hydrogel nanofibers, AFG: aligned fibrin hydrogel nanofibers. (b) Images of regenerated nerve fibers isolated from middle of the implanted site at 12 weeks after surgery. Toluidine blue-stained transverse sections (top) and transmission electron microscopy (TEM) images (middle and bottom) of the regenerated sciatic nerve. Reproduced from Du et al.[62] (c) Processes of spinal cord injury repair study using fibrous GelMA scaffold. (d) Evaluation of rat limb motor function with Basso, Beattie, and Bresnahan (BBB) score after implantation of the GelMA scaffold. Reproduced from Chen et al.[63]

expected to inhibit hypertrophic scar formation. As a result, the dressings promoted wound healing and relatively inhibited scar formation. Additionally, angiogenesis regarded as an indicator of scar formation[123,124] was reduced when the dressings were used to treat wounds (Figure 11(f)).

Wounds at skins were effectively treated with electrospun fibrous hydrogel-based wound dressings developed with healing strategies, showing potential to treat various types of wounds at skins. Development of diverse target-specific healing strategies as well as relatively easy
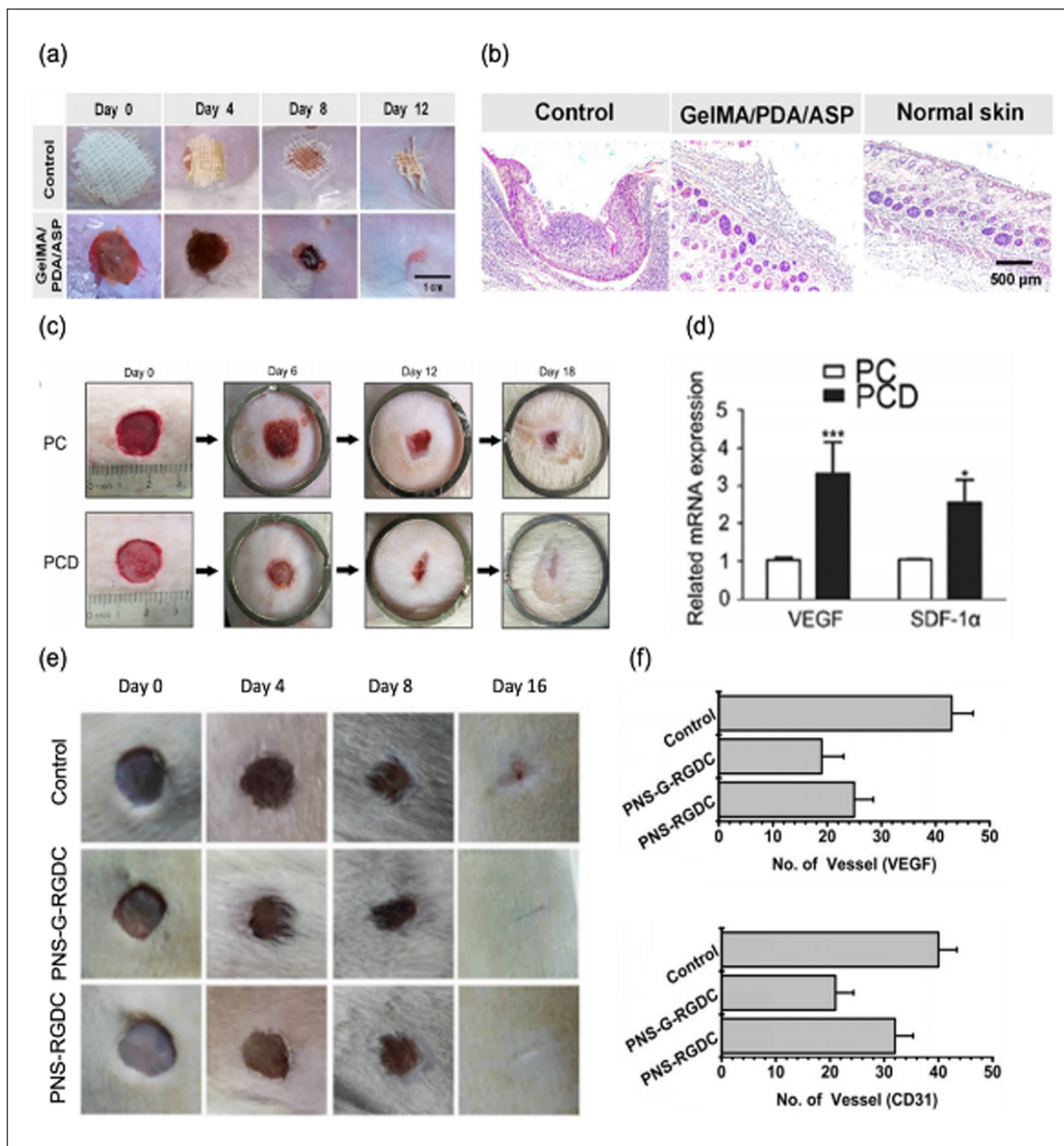
Figure 11. Wound dressings developed with fibrous hydrogels. (a) Pictures of wounds covered with gauze (Control) and GelMA-PDA-ASP nanofibers on day 0, 4, 8, and 12. (b) H&E images of sectioned wound site after 12 days of treatment. Reproduced from Zhang et al.[64] (c) Pictures of wounds treated with PVA/CS (PC) nanofibers or PC nanofibers loaded with DFO (PCD) on diabetic rats on day 0, 6, 12, and 18. (d) mRNA expression of VEGF and SDF-1α after 6 days of PC and PCD treatment. Reproduced from Chen et al.[65] (e) Pictures of the wounds from control, PNS microfibers with GS-Rg3 and cell adhesion peptide (PNS-G-RGDC) and PNS microfibers with cell adhesion peptide (PNS-RGDC) groups on day 0, 4, 8, and 16. (f) Immunohistochemical staining analysis of VEGF (top) and CD31 (bottom) after 16 days of treatment. Reproduced from Xu et al.[66]
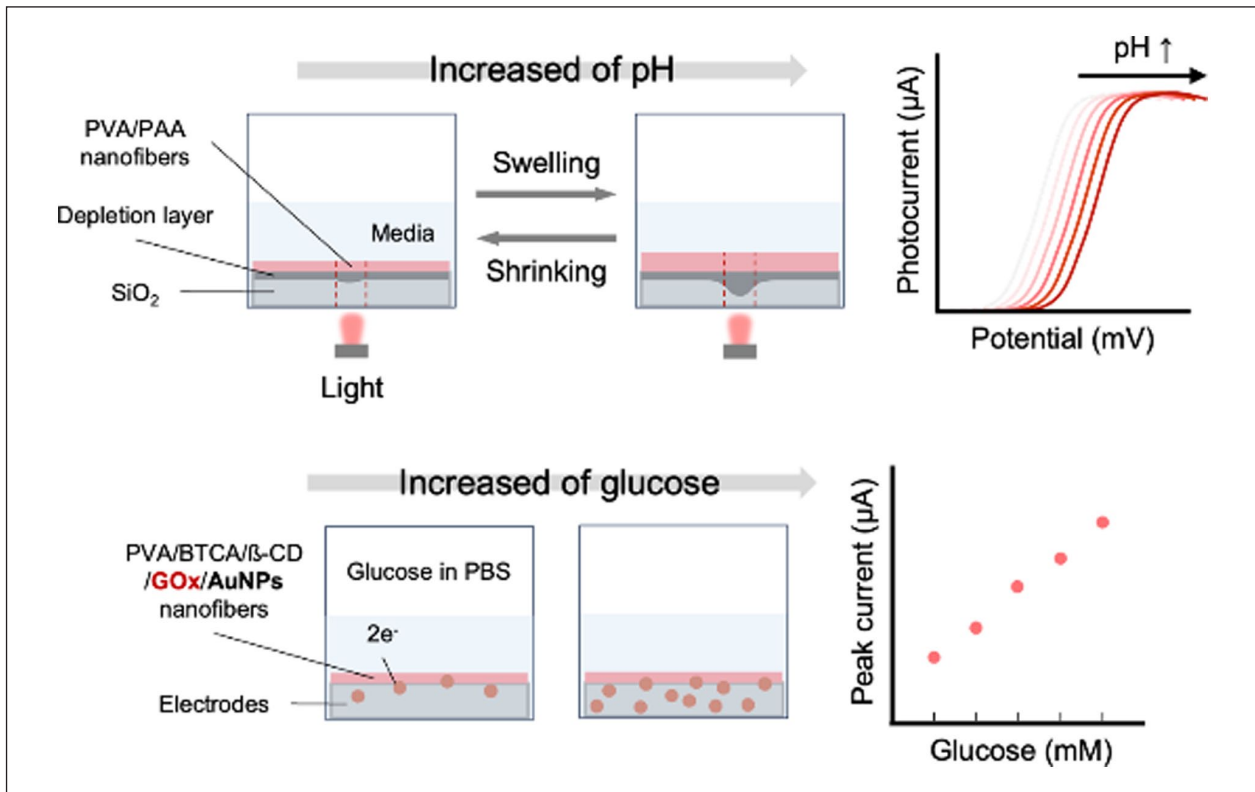
Figure 12. Illustration of working principles of pH-sensitive and glucose-sensitive biosensors fabricated with fibrous hydrogels.

fabrication methods might be useful for wide application of these electrospun fibrous hydrogel-based dressings.

PH- and glucose-sensitive biosensors

Conventionally, hydrogel-based biosensors can detect biological events in two different ways.[125] The first one uses stimulus (e.g. pH, temperature, and electrical field)-sensitive changes in hydrogel swelling degrees for the sensing of biological events. In the other way, the biological events were detected via using bioreceptors that were added to hydrogels and categorized as enzyme, antibody, biomimetic, cell, and DNA.[125] Likewise, biosensors fabricated with fibrous hydrogels and used for biomedical applications also worked with these principles.

Specifically, working principles of fibrous hydrogel-based biosensors that were sensitive to pH and glucose are described in Figure 12. The pH-responsive biosensors were working with pH-sensitive swelling/deswelling of PVA/PAA nanofibers. In response to variation of media pH, the sensitive layer (PVA/PAA nanofibers) of the biosensor swelled/deswelled and capacitance of the layer varied. As a result, changes of media pH could vary photocurrents under light exposure. For the glucose responsive biosensors, the glucose oxidase enzyme was encapsulated in fibrous hydrogels. Thus, the currents could be increased via oxidation when there was glucose. In this case, the enzyme was used as a bioreceptor.

As applications, PVA/PAA nanofibers sensitive to pH were integrated with a light addressable potentiometric

sensor (LAPS) (NF-LAPS) to measure acidification of cancer cells and response of them to drugs (Figure 13(a)).[68] As a result, the NF-LAPS was able to sense variation of extracellular acidification when concentration of cancer cells in glucose-rich media was varied (Figure 13(b)). Additionally, effects of doxorubicin and enzyme inhibitors alone or together on cancer cells resistant to some drugs were verified by measuring variation of extracellular acidification.

Additionally, patch sensor developed with PVA/BTCA/β-CD/GOx/AuNPs nanofibers were used to measure concentration of glucose (Figure 13(c)).[69] Enzymatic activity of those nanofibers was maintained relatively high via GOx/β-CD inclusion complex and AuNPs although their fabrication processes involved using high voltage and temperature (Figure 13(d)). It appears that structures and sizes of electrospun hydrogel nanofibers, compared to those of bulk hydrogels, helped enhancing performance of sensors. Similar to aforementioned hydrogel nanofiber-based applications, sensors with various practical functions for biomedical applications are expected if diverse characteristics of hydrogels in electrospun nanofiber forms are exploited for development of biosensors.

Future outlook

Various polymers, other than hydrogels, have been used for electrospinning to obtain polymeric micro/nanofibers
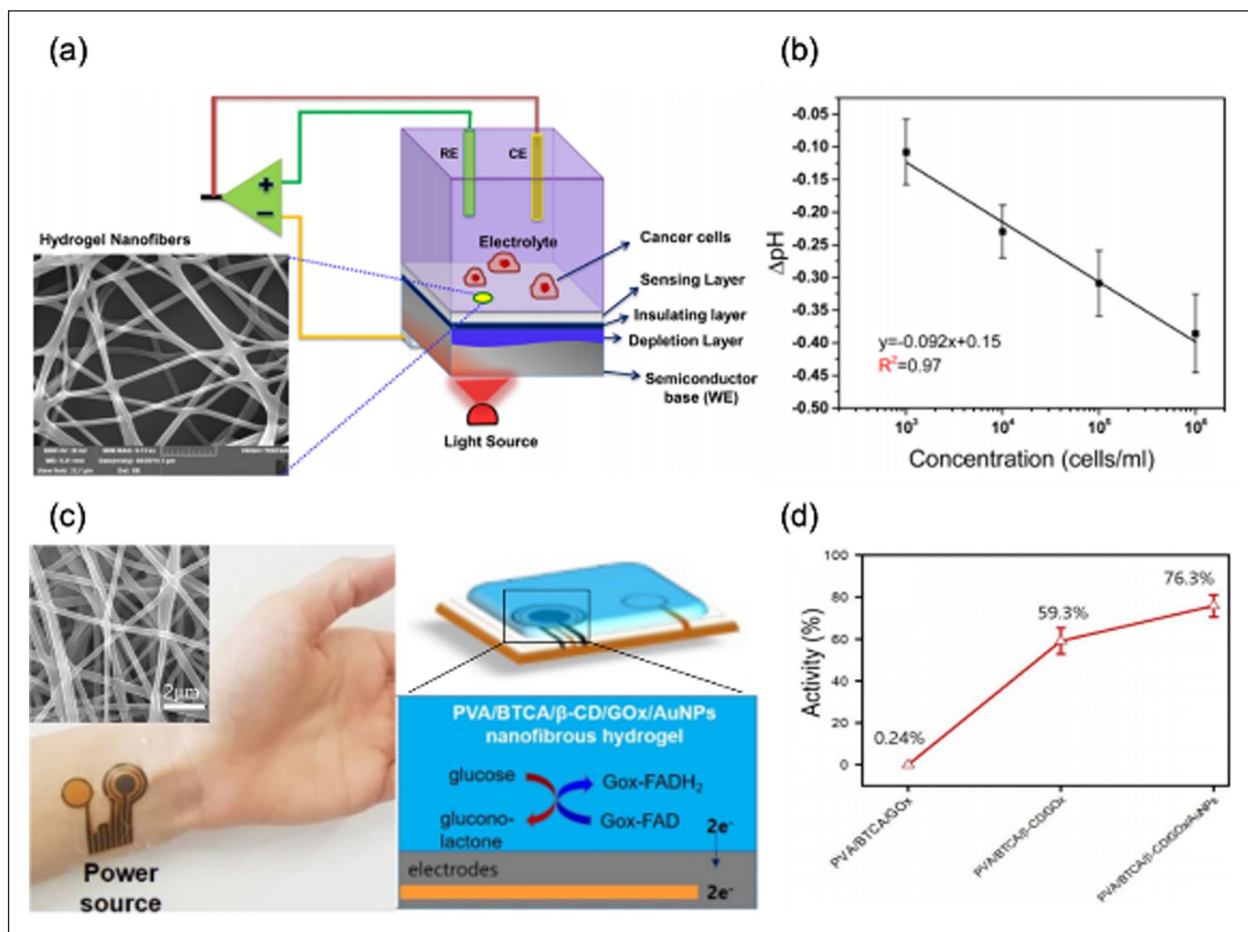
Figure 13. Biosensors developed with electrospun fibrous hydrogels. (a) A structure of a light addressable potentiometric sensor integrated with PVA/PAA nanofibers (NF-LAPS). (b) Measurement of pH shift with varied concentration of cancer cells. Reproduced from Shaibani et al.[68] (c) A wearable biosensor fabricated with PVA/BTCA/β-CD/GOx/AuNPs hydrogel nanofibers. (d) Analysis of enzymatic activity of PVA/BTCA/GOx, PVA/BTCA/β-CD/GOx, and PVA/BTCA/β-CD/GOx/AuNPs hydrogel nanofibers. Reproduced from Kim and Kim.[69] Distributed under the Creative Commons Attribution License 4.0 (CCBY, http://creativecommons.org/licenses/by/4.0).
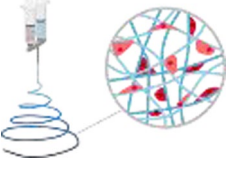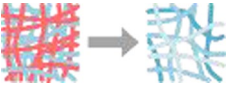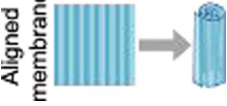
mimicking geometries of ECM, and those fibers have been intensively used for various biomedical applications. In particular, PCL fibers, relatively easy to fabricate, biocompatible and degradable, have shown great outcomes in biomedical fields although their stiffness and adhesiveness to cells were quite different from those features of natural ECM. Recently, hydrogels that exhibited their ability to mimic various characteristics of ECM were used to fabricate micro/nanofibers, and studies used those fibers have shown distinct cellular behaviors and responses that were not known before. Especially, fabrication of fibers soft enough for cells to deform and remodel allowed to study how stiffness of fibers could affect cells, and cellular behaviors and responses were significantly influenced by fiber stiffness. These clearly implied that fibrous hydrogels have potential to draw great outcomes in biomedical fields by exploiting various characteristics and easy modification of hydrogels.

In 2D/3D cell culture systems, fibrous hydrogels might be able to provide ECM-like environment by modifying their stiffness, adhesiveness to cells, degradability and growth factor presentation in addition to geometry and topography. Strategies permitting cell migration through fibrous hydrogels via deformation and degradation of fibers can be useful for 3D cell culture. Tightly stacked fibers and fragmented fibers linked with non-degradable crosslinkers might not be ideal for culturing encapsulated cells. The strategies enhancing cell migration through fibrous hydrogels, which can vary through target tissues or type of diseases, can be also applied to implantable scaffolds and wound dressings for rapid tissue regeneration. Various hydrogels displaying stimuli-sensitive responses can be applied for development of sensors performing biomedical functions with precise measurement.

On the other hand, there exist some limitations on electrospun fibrous hydrogels developed for biomedical applications. For instance, productivities of electrospinning techniques used for fabrication of fibrous hydrogels were low because flow rates of hydrogel precursors were mostly

Table 4. Methods for fabricating 3D environments with fibrous hydrogels, control of physical properties of the fibrous hydrogels and biomedical applications of the 3D environments.

Methods	Control of physical properties	Biomedical applications	Ref.
Wet electrospinning	-	3D cell culture platform for mesenchymal stem cells	Majidi et al.[23]
Cell-loaded electrospinning	-	3D cell culture platform for NIH 3T3 fibroblast or C2C12 myoblasts cells	Xu et al.[59]
Removal of sacrificial fibers in fiber networks	Porosity of scaffold - Ratio of sacrificial fibers in fiber networks	Tissue-engineered scaffold for regeneration of dense connective tissue	Qu et al.[61]
Assembly of fragmented fibers	Contractability - Concentration of fragmented fibers	3D printed 3D cell culture platform for mesenchymal stem cells	Davidson et al.[60]
	Porosity of scaffold - Spacing of 3D printed strand	3D printed tissue-engineered scaffold for regeneration of cartilage	Chen et al.[67]
	Porosity of scaffold - Concentration of fragmented fibers	3D electrospun fibrous sponge for potential regeneration scaffolds	Li et al.[126]
Rolling of fiber membranes	Alignment of fibers - Customized collector	Scaffolds to guide axonal regeneration	Chen et al.[63]
	Alignment of fibers - Speed of rotating collector	Scaffolds to guide axonal regeneration	Du et al.[62]
Subcritical CO_2 fluid	-	3D patterned scaffold for wound dressings in diabetic	Li et al.[22]

low during the fabrication processes. Needless electrospinning technique, of course, enhanced productivity by generating multiple jets.[24] In addition, fibrous hydrogels in many researches were collected as densely packed mat forms that often limited cell infiltration through fibers and cell encapsulation within fiber networks. Likewise, some techniques to generate 3D environments with fibrous hydrogels (described in Table 4) were developed to improve this issue.[22,23,59–63,67,126] Lastly, solvents toxic to cells were used for fabrication of some fibrous hydrogels. To ensure biocompatibility of fibrous hydrogels, removal of solvents were performed via washing with PBS[63] or drying steps.[22,66,67]

Overall, fibrous hydrogels fabricated with electrospinning techniques in recent studies have shown great potential in biomedical applications. Exploiting diverse characteristics of hydrogels and developing efficient strategies would be useful to expand their biomedical applications and enhance their performances.

Conclusion

Polymeric micro/nanofibers mimicking geometries of ECM have been fabricated with electrospinning techniques and intensively used for various biomedical applications. In particular, various hydrogels that can be modified to mimic diverse ECM features were also used to generate electrospun hydrogel fibers, and the fibrous hydrogels were applied to biomedical fields. For instance, fibrous hydrogels fabricated with electrospinning techniques were used to develop 2D/3D cell culture platforms to study cellular behaviors and responses, implantable

scaffolds to regenerate tissues and wound dressings to enhance recovery of wounded skin. In addition, fibrous hydrogels sensitive to stimuli were used to develop biosensors. Overall, fibrous hydrogels have exhibited great performances within those biomedical applications. In the future, applications of the fibrous hydrogels in biomedical fields can be expanded through exploiting various characteristics of hydrogels, modifying their compositions and developing effective strategies.

Author contributions

J.W.L. investigated review contents and wrote original draft. K.H.S. supervised writing this review and reviewed and edited the draft.

Declaration of conflicting interests

The author(s) declared no potential conflicts of interest with respect to the research, authorship, and/or publication of this article.

Funding

ORCID iD

Kwang Hoon Song https://orcid.org/0000-0001-8143-7148

References

1. Frantz C, Stewart KM and Weaver VM. The extracellular matrix at a glance. *J Cell Sci* 2010; 123: 4195–4200.
2. Chen Y, Lee K, Kawazoe N, et al. ECM scaffolds mimicking extracellular matrices of endochondral ossification for the regulation of mesenchymal stem cell differentiation. *Acta Biomater* 2020; 114: 158–169.
3. Geckil H, Xu F, Zhang X, et al. Engineering hydrogels as extracellular matrix mimics. *Nanomed* 2010; 5: 469–484.
4. Zhu C, Lei H, Fan D, et al. Novel enzymatic crosslinked hydrogels that mimic extracellular matrix for skin wound healing. *J Mater Sci* 2018; 53: 5909–5928.
5. Lee KY and Mooney DJ. Hydrogels for tissue engineering. *Chem Rev* 2001; 101: 1869–1879.
6. Li X, Sun Q, Li Q, et al. Functional hydrogels with tunable structures and properties for tissue engineering applications. *Front Chem* 2018; 6: 499.
7. Catoira MC, Fusaro L, Di Francesco D, et al. Overview of natural hydrogels for regenerative medicine applications. *J Mater Sci Mater Med* 2019; 30(10): 115.
8. Meyvis TKL, De Smedt SC, Demeester J, et al. Influence of the degradation mechanism of hydrogels on their elastic and swelling properties during degradation. *Macromolecules* 2000; 33: 4717–4725.
9. Farino Reyes CJ, Pradhan S and Slater JH. The influence of ligand density and degradability on hydrogel induced

breast cancer dormancy and reactivation. *Adv Healthc Mater* 2021; 10: e2002227.
10. Clevenger TN, Luna G, Boctor D, et al. Cell-mediated remodeling of biomimetic encapsulating hydrogels triggered by adipogenic differentiation of adipose stem cells. *J Tissue Eng* 2016; 7: 2041731416670482.
11. Hagiwara M, Maruyama H, Akiyama M, et al. Weakening of resistance force by cell-ECM interactions regulate cell migration directionality and pattern formation. *Commun biol* 2021; 4: 808.
12. Gaudet C, Marganski WA, Kim S, et al. Influence of type I collagen surface density on fibroblast spreading, motility, and contractility. *Biophys J* 2003; 85: 3329–3335.
13. Koohestani F, Braundmeier AG, Mahdian A, et al. Extracellular matrix collagen alters cell proliferation and cell cycle progression of human uterine leiomyoma smooth muscle cells. *PLoS One* 2013; 8: e75844.
14. Chi HY, Chan V, Li C, et al. Fabrication of polylactic acid/paclitaxel nano fibers by electrospinning for cancer therapeutics. *BMC chem* 2020; 14(1): 63.
15. Matera DL, DiLillo KM, Smith MR, et al. Microengineered 3D pulmonary interstitial mimetics highlight a critical role for matrix degradation in myofibroblast differentiation. *Sci Adv* 2020; 6: eabb5069.
16. Liu R, Xu X, Zhuang X, et al. Solution blowing of chitosan/PVA hydrogel nanofiber mats. *Carbohydr Polym* 2014; 101: 1116–1121.
17. Nilsson TY and Trojer MA. A solution blown superporous nonwoven hydrogel based on hydroxypropyl cellulose. *Soft Matter* 2020; 16: 6850–6861.
18. Hwang W, Kim B-H, Dandu R, et al. Surface induced nanofiber growth by self-assembly of a silk-elastin-like protein polymer. *Langmuir* 2009; 25: 12682–12686.
19. Sant S, Coutinho DF, Gaharwar AK, et al. Self-assembled hydrogel fiber bundles from oppositely charged polyelectrolytes mimic micro-/nanoscale hierarchy of collagen. *Adv Funct Mater* 2017; 27: 1606273.
20. Coleman BF, Street RM, Fitzsimons T, et al. Touchspinning: mechanically drawing polyacrylonitrile nanofibers. *J Appl Polym Sci* 2022; 139: 52339.
21. Park S, Yuk H, Zhao R, et al. Adaptive and multifunctional hydrogel hybrid probes for long-term sensing and modulation of neural activity. *Nat Commun* 2021; 12: 3435.
22. Li J, Zhang T, Pan M, et al. Nanofiber/hydrogel coreshell scaffolds with three-dimensional multilayer patterned structure for accelerating diabetic wound healing. *Nanobiotechnol* 2022; 20: 28–18.
23. Majidi SS, Slemming-Adamsen P, Hanif M, et al. Wet electrospun alginate/gelatin hydrogel nanofibers for 3D cell culture. *Int J Biol Macromol* 2018; 118: 1648–1654.
24. Cengiz-çallıoğlu F. Dextran nanofiber production by needleless electrospinning process. *e-Polymers* 2014; 14: 5–13.
25. Silva MJ, Dias YJ and Yarin AL. Electrically-assisted supersonic solution blowing and solution blow spinning of fibrous materials from natural rubber extracted from havea brasilienses. *Ind Crops Prod* 2023; 192: 116101.
26. Elnabawy E, Farag M, Soliman A, et al. Solution blow spinning of piezoelectric nanofiber mat for detecting mechanical and acoustic signals. *J Appl Polym Sci* 2021; 138: 51322.

27. Gao Y, Zhang J, Su Y, et al. Recent progress and challenges in solution blow spinning. *Mater Horiz* 2021; 8: 426–446.

28. Zheng W and Wang X. Effects of cylindrical-electrode-assisted solution blowing spinning process parameters on polymer nanofiber morphology and microstructure. *e-Polymers* 2019; 19: 190–202.

29. Tan C, Qi X, Liu Z, et al. Self-assembled chiral nanofibers from ultrathin low-dimensional nanomaterials. *J Am Chem Soc* 2015; 137: 1565–1571.

30. Zagorodko O, Melnyk T, Rogier O, et al. Higher-order interfiber interactions in the self-assembly of benzene-1,3,5-tricarboxamide-based peptides in water. *Polym Chem* 2021; 12: 3478–3487.

31. Shen Y, Wang Z, Wang Z, et al. Thermally drawn multifunctional fibers: toward the next generation of information technology. *InfoMat* 2022; 4: e12318.

32. Can-Herrera LA, Oliva AI, Dzul-Cervantes MAA, et al. Morphological and mechanical properties of electrospun polycaprolactone scaffolds: effect of applied voltage. *Polymers* 2021; 13: 662.

33. Zargham S, Bazgir S, Tavakoli A, et al. The effect of flow rate on morphology and deposition area of electrospun nylon 6 nanofiber. *J Eng Fiber Fabr* 2012; 7: 155892501200700400.

34. Singh YP, Dasgupta S, Nayar S, et al. Optimization of electrospinning process & parameters for producing defect-free chitosan/polyethylene oxide nanofibers for bone tissue engineering. *J Biomater Sci Polym Ed* 2020; 31: 781–803.

35. Hodgkinson T, Yuan X-F and Bayat A. Electrospun silk fibroin fiber diameter influences in vitro dermal fibroblast behavior and promotes healing of ex vivo wound models. *J Tissue Eng* 2014; 5: 2041731414551661.

36. Tiwari SK and Venkatraman SS. Importance of viscosity parameters in electrospinning: of monolithic and core–shell fibers. *Mater Sci Eng C* 2012; 32: 1037–1042.

37. Robinson AJ, Pérez-Nava A, Ali SC, et al. Comparative analysis of fiber alignment methods in electrospinning. *Matters* 2021; 4: 821–844.

38. Gnavi S, Fornasari BE, Tonda-Turo C, et al. The effect of electrospun gelatin fibers alignment on schwann cell and axon behavior and organization in the perspective of artificial nerve design. *Int J Mol Sci* 2015; 16: 12925–12942.

39. Cai X, Zhu P, Lu X, et al. Electrospinning of very long and highly aligned fibers. *J Mater Sci* 2017; 52: 14004–14010.

40. Yang D, Zhang J, Zhang J, et al. Aligned electrospun nanofibers induced by magnetic field. *J Appl Polym Sci* 2008; 110: 3368–3372.

41. Rahman SU, Ponnusamy S, Nagrath M, et al. Precision-engineered niche for directed differentiation of MSCs to lineage-restricted mineralized tissues. *J Tissue Eng* 2022; 13: 20417314211073934.

42. Cipitria A, Skelton A, Dargaville TR, et al. Design, fabrication and characterization of PCL electrospun scaffolds—a review. *J Mater Chem* 2011; 21: 9419–9453.

43. Huang Y, Shi R, Gong M, et al. Icariin-loaded electrospun PCL/gelatin sub-microfiber mat for preventing epidural adhesions after laminectomy. *Int J Nanomedicine* 2018; 13: 4831–4844.

44. Zhao L, Li X, Yang L, et al. Evaluation of remodeling and regeneration of electrospun PCL/fibrin vascular grafts in vivo. *Mater Sci Eng C* 2021; 118: 111441.

45. Maleki H, Azimi B, Ismaeilimoghadam S, et al. Poly (lactic acid)-based electrospun fibrous structures for biomedical applications. *Appl Sci* 2022; 12: 3192.

46. Fang Y, Zhu X, Wang N, et al. Biodegradable core-shell electrospun nanofibers based on PLA and γ-PGA for wound healing. *Eur Polym J* 2019; 116: 30–37.

47. Zhao W, Li J, Jin K, et al. Fabrication of functional PLGA-based electrospun scaffolds and their applications in biomedical engineering. *Mater Sci Eng C* 2016; 59: 1181–1194.

48. Kim M-J, Kim J-H, Yi G, et al. In vitro andin vivo application of PLGA nanofiber for artificial blood vessel. *Macromol Res* 2008; 16: 345–352.

49. Lee CH, Huang SC, Hung KC, et al. Enhanced diabetic wound healing using electrospun biocompatible PLGA-based saxagliptin fibrous membranes. *Nanomater* 2022; 12: 3740.

50. Chor A, Takiya CM, Dias ML, et al. In vitro and in vivo cell-interactions with electrospun poly (lactic-co-glycolic acid) (PLGA): morphological and immune response analysis. *Polymers* 2022; 14: 4460.

51. Kucinska-Lipka J, Gubanska I, Janik H, et al. Fabrication of polyurethane and polyurethane based composite fibres by the electrospinning technique for soft tissue engineering of cardiovascular system. *Mater Sci Eng C* 2015; 46: 166–176.

52. Gostev AA, Shundrina IK, Pastukhov VI, et al. In vivo stability of polyurethane-based electrospun vascular grafts in terms of chemistry and mechanics. *Polymers* 2020; 12: 845.

53. Sheikholeslam M, Wright MEE, Cheng N, et al. Electrospun polyurethane-gelatin composite: a new tissue-engineered scaffold for application in skin regeneration and repair of complex wounds. *ACS Biomater Sci Eng* 2020; 6: 505–516.

54. Dubal S and Chavan S. Electrospun polyacrylonitrile carbon nanofiber for supercapacitor application: a review. In: Kragh MK, Nedelcu D, Belouettar S et al. (eds) *Advanced engineering forum*. Trans Tech Publ, 2021, pp.25–42.

55. Malik S, Sundarrajan S, Hussain T, et al. Fabrication of highly oriented cylindrical polyacrylonitrile, poly(lactide-co-glycolide), polycaprolactone and poly(vinyl acetate) nanofibers for vascular graft applications. *Polymers* 2021; 13: 2075.

56. Baker BM, Trappmann B, Wang WY, et al. Cell-mediated fibre recruitment drives extracellular matrix mechano-sensing in engineered fibrillar microenvironments. *Nat Mater* 2015; 14: 1262–1268.

57. Nie K, Han S, Yang J, et al. Enzyme-crosslinked electrospun fibrous gelatin hydrogel for potential soft tissue engineering. *Polymers* 2020; 12: 1977.

58. Davidson MD, Song KH, Lee M-H, et al. Engineered fibrous networks to investigate the influence of fiber mechanics on myofibroblast differentiation. *ACS Biomater Sci Eng* 2019; 5: 3899–3908.

59. Xu F, Dodd M, Sheardown H, et al. Single-step reactive electrospinning of cell-loaded nanofibrous scaffolds as ready-to-use tissue patches. *Biomacromolecules* 2018; 19: 4182–4192.

60. Davidson MD, Prendergast ME, Ban E, et al. Programmable and contractile materials through cell encapsulation in fibrous hydrogel assemblies. *Sci Adv* 2021; 7: eabi8157.

61. Qu F, Holloway JL, Esterhai JL, et al. Programmed biomolecule delivery to enable and direct cell migration for connective tissue repair. *Nat Commun* 2017; 8: 1780.

62. Du J, Liu J, Yao S, et al. Prompt peripheral nerve regeneration induced by a hierarchically aligned fibrin nanofiber hydrogel. *Acta Biomater* 2017; 55: 296–309.

63. Chen C, Tang J, Gu Y, et al. Bioinspired hydrogel electrospun fibers for spinal cord regeneration. *Adv Funct Mater* 2019; 29: 1806899.

64. Zhang K, Lv H, Zheng Y, et al. Nanofibrous hydrogels embedded with phase-change materials: temperature-responsive dressings for accelerating skin wound healing. *Compos Commun* 2021; 25: 100752.

65. Chen H, Jia P, Kang H, et al. Upregulating hif-1α by hydrogel nanofibrous scaffolds for rapidly recruiting angiogenesis relative cells in diabetic wound.. *Adv Healthc Mater* 2016; 5: 907–918.

66. Xu T, Yang R, Ma X, et al. Bionic poly(γ-glutamic acid) electrospun fibrous scaffolds for preventing hypertrophic scars. *Adv Healthc Mater* 2019; 8: e1900123.

67. Chen W, Xu Y, Liu Y, et al. Three-dimensional printed electrospun fiber-based scaffold for cartilage regeneration. *Mater Des* 2019; 179: 107886.

68. Shaibani PM, Etayash H, Naicker S, et al. Metabolic study of cancer cells using a pH sensitive hydrogel nanofiber light addressable potentiometric sensor. *ACS Sens* 2017; 2: 151–156.

69. Kim GJ and Kim KO. Novel glucose-responsive of the transparent nanofiber hydrogel patches as a wearable biosensor via electrospinning. *Sci Rep* 2020; 10: 18858.

70. Li D and Xia Y. Electrospinning of nanofibers: reinventing the wheel? *Adv Mater* 2004; 16: 1151–1170.

71. Xue J, Wu T, Dai Y, et al. Electrospinning and electrospun nanofibers: methods, materials, and applications. *Chem Rev* 2019; 119: 5298–5415.

72. Chanunpanich N, Lee B and Byun H. A study of electrospun PVDF on PET sheet. *Macromol Res* 2008; 16: 212–217.

73. Ferrández-Rives M, Beltrán-Osuna ÁA, Gómez-Tejedor JA, et al. Electrospun PVA/bentonite nanocomposites mats for drug delivery. *Materials* 2017; 10: 1448.

74. Ryu HI, Koo MS, Kim S, et al. Uniform-thickness electrospun nanofiber mat production system based on real-time thickness measurement. *Sci Rep* 2020; 10: 20847.

75. Calhoun MA, Chowdhury SS, Nelson MT, et al. Effect of electrospun fiber mat thickness and support method on cell morphology. *Nanomater* 2019; 9: 644.

76. Rnjak-Kovacina J, Wise SG, Li Z, et al. Tailoring the porosity and pore size of electrospun synthetic human elastin scaffolds for dermal tissue engineering. *Biomaterials* 2011; 32: 6729–6736.

77. Vitale A, Massaglia G, Chiodoni A, et al. Tuning porosity and functionality of electrospun rubber nanofiber mats by photo-crosslinking. *ACS Appl Mater Interfaces* 2019; 11: 24544–24551.

78. Mahjour SB, Sefat F, Polunin Y, et al. Improved cell infiltration of electrospun nanofiber mats for layered tissue constructs. *J Biomed Mater Res A* 2016; 104: 1479–1488.

79. Han T, Reneker DH and Yarin AL. Buckling of jets in electrospinning. *Polymer* 2007; 48: 6064–6076.

80. Marginean I, Parvin L, Heffernan L, et al. Flexing the electrified meniscus: the birth of a jet in electrosprays. *Anal Chem* 2004; 76: 4202–4207.

81. Han D and Steckl AJ. Coaxial electrospinning formation of complex polymer fibers and their applications. *ChemPlusChem* 2019; 84: 1453–1497.

82. Xu Y, Guo P and Akono A-T. Novel wet electrospinning inside a reactive pre-ceramic gel to yield advanced nanofiber-reinforced geopolymer composites. *Polymers* 2022; 14: 3943.

83. Partheniadis I, Nikolakakis I, Laidmäe I, et al. A minireview: needleless electrospinning of nanofibers for pharmaceutical and biomedical applications. *Processes* 2020; 8: 673.

84. Tomal W and Ortyl J. Water-soluble photoinitiators in biomedical applications. *Polymers* 2020; 12: 1073.

85. Chyzy A, Tomczykowa M and Plonska-Brzezinska ME. Hydrogels as potential nano-, micro- and macro-scale systems for controlled drug delivery. *Materials* 2020; 13: 188.

86. Jang MJ, Bae SK, Jung YS, et al. Enhanced wound healing using a 3D printed VEGF-mimicking peptide incorporated hydrogel patch in a pig model. *Biomed Mater* 2021; 16: 045013.

87. Li H, Tan C and Li L. Review of 3D printable hydrogels and constructs. *Mater Des* 2018; 159: 20–38.

88. Kasahara Y, Sato Y, Masukawa MK, et al. Photolithographic shape control of DNA hydrogels by photo-activated self-assembly of DNA nanostructures. *APL Bioeng* 2020; 4: 016109.

89. He J, Zhu L, Liu Y, et al. Sequential assembly of 3D perfusable microfluidic hydrogels. *J Mater Sci Mater Med* 2014; 25: 2491–2500.

90. Emerson AE, McCall AB, Brady SR, et al. Hydrogel injection molding to generate complex cell encapsulation geometries. *ACS Biomater Sci Eng* 2022; 8: 4002–4013.

91. Ilhan E, Cesur S, Sulutas RB, et al. The role of Multilayer Electrospun poly(vinyl alcohol)/gelatin nanofibers loaded with fluconazole and cinnamaldehyde in the potential treatment of fungal keratitis. *Eur Polym J* 2022; 176: 111390.

92. Davidson MD, Ban E, Schoonen ACM, et al. Mechanochemical adhesion and plasticity in multifiber hydrogel networks. *Adv Mater* 2020; 32: e1905719.

93. Kumari J, Wagener FADTG and Kouwer PHJ. Novel synthetic polymer-based 3D contraction assay: a versatile preclinical research platform for fibrosis. *ACS Appl Mater Interfaces* 2022; 14: 19212–19225.

94. Chan V, Park K, Collens MB, et al. Development of miniaturized walking biological machines. *Sci Rep* 2012; 2: 857.

95. Castillo Diaz LA, Elsawy M, Saiani A, et al. Osteogenic differentiation of human mesenchymal stem cells promotes mineralization within a biodegradable peptide hydrogel. *J Tissue Eng* 2016; 7: 2041731416649789.

96. Ding Y, Xu X, Sharma S, et al. Biomimetic soft fibrous hydrogels for contractile and pharmacologically responsive smooth muscle. *Acta Biomater* 2018; 74: 121–130.

97. Wang B, Wang L, Tang Y, et al. Fabrication of spaced monolayers of electrospun nanofibers for three-dimensional cell infiltration and proliferation. *Microelectron Eng* 2018; 198: 73–77.

98. Sun X, Lang Q, Zhang H, et al. Cell Scaffolds: Electrospun photocrosslinkable hydrogel fibrous scaffolds for rapid in vivo vascularized skin flap regeneration. *Adv Funct Mater* 2017; 27: 1604617.

99. Contessi Negrini N, Tarsini P, Tanzi MC, et al. Chemically crosslinked gelatin hydrogels as scaffolding materials for adipose tissue engineering. *J Appl Polym Sci* 2019; 136: 47104.

100. Mohand-Kaci F, Assoul N, Martelly I, et al. Optimized hyaluronic acid-hydrogel design and culture conditions for preservation of mesenchymal stem cell properties. *Tissue Eng Part C Methods* 2013; 19: 288–298.

101. Kim Y-J, Tachibana M, Umezu M, et al. Bio-inspired smart hydrogel with temperature-dependent properties and enhanced cell attachment. *J Mater Chem B* 2016; 4: 1740–1746.

102. Athirasala A, Lins F, Tahayeri A, et al. A novel strategy to engineer pre-vascularized full-length dental pulp-like tissue constructs. *Sci Rep* 2017; 7(1): 11.

103. Xue B, Tang D, Wu X, et al. Engineering hydrogels with homogeneous mechanical properties for controlling stem cell lineage specification. *Proc Natl Acad Sci* 2021; 118: e2110961118.

104. Xia J, Liu Z-Y, Han Z-Y, et al. Regulation of cell attachment, spreading, and migration by hydrogel substrates with independently tunable mesh size. *Acta Biomater* 2022; 141: 178–189.

105. Kim D-S, Kim JH, Baek S-W, et al. Controlled vitamin D delivery with injectable hyaluronic acid-based hydrogel for restoration of tendinopathy. *J Tissue Eng* 2022; 13: 20417314221122089.

106. Scelsi A, Bochicchio B, Smith A, et al. Tuning of hydrogel stiffness using a two-component peptide system for mammalian cell culture. *J Biomed Mater Res A* 2019; 107: 535–544.

107. Sun Y, Deng R, Ren X, et al. 2D gelatin methacrylate hydrogels with tunable stiffness for investigating cell behaviors. *ACS appl bio mater* 2019; 2: 570–576.

108. Cosson S and Lutolf MP. Hydrogel microfluidics for the patterning of pluripotent stem cells. *Sci Rep* 2014; 4(1): 6.

109. Hsieh H-Y, Camci-Unal G, Huang T-W, et al. Gradient static-strain stimulation in a microfluidic chip for 3D cellular alignment. *Lab Chip* 2014; 14: 482–493.

110. Dou J, Mao S, Li H, et al. Combination stiffness gradient with chemical stimulation directs glioma cell migration on a microfluidic chip. *Anal Chem* 2020; 92: 892–898.

111. Tunesi M, Izzo L, Raimondi I, et al. A miniaturized hydrogel-based in vitro model for dynamic culturing of human cells overexpressing beta-amyloid precursor protein. *J Tissue Eng* 2020; 11: 2041731420945633.

112. Nie J, Gao Q, Wang Y, et al. Vessel-on-a-chip with hydrogel-based microfluidics. *Small* 2018; 14: e1802368.

113. Meng Q, Wang Y, Li Y, et al. Hydrogel microfluidic-based liver-on-a-chip: mimicking the mass transfer and structural features of liver. *Biotechnol Bioeng* 2021; 118: 612–621.

114. Kim IL, Khetan S, Baker BM, et al. Fibrous hyaluronic acid hydrogels that direct MSC chondrogenesis through mechanical and adhesive cues. *Biomaterials* 2013; 34: 5571–5580.

115. Liang J, Chen H, Guo Z, et al. Tough fibrous mats prepared by electrospinning mixtures of methacrylated poly(trimethylene carbonate) and methacrylated gelatin. *Eur Polym J* 2021; 152: 110471.

116. Guimarães A, Martins A, Pinho ED, et al. Solving cell infiltration limitations of electrospun nanofiber meshes for tissue engineering applications. *Nanomed* 2010; 5: 539–554.

117. Tonsomboon K and Oyen ML. Composite electrospun gelatin fiber-alginate gel scaffolds for mechanically robust tissue engineered cornea. *J Mech Behav Biomed Mater* 2013; 21: 185–194.

118. Nguyen AV and Soulika AM. The dynamics of the skin's immune system. *Int J Mol Sci* 2019; 20: 1811.

119. Rezvani Ghomi E, Khalili S, Nouri Khorasani S, et al. Wound dressings: current advances and future directions. *J Appl Polym Sci* 2019; 136: 47738.

120. Dong Y, Zheng Y, Zhang K, et al. Electrospun nanofibrous materials for wound healing. *Adv Fiber Mater* 2020; 2: 212–227.

121. Mogoşanu GD and Grumezescu AM. Natural and synthetic polymers for wounds and burns dressing. *Int J Pharm* 2014; 463: 127–136.

122. D'Amico R, Malucelli C, Uccelli A, et al. Therapeutic arteriogenesis by factor-decorated fibrin matrices promotes wound healing in diabetic mice. *J Tissue Eng* 2022; 13: 20417314221119615.

123. Kwak DH, Bae TH, Kim WS, et al. Anti-vascular endothelial growth factor (Bevacizumab) therapy reduces hypertrophic scar formation in a rabbit ear wounding model. *Arch Plast Surg* 2016; 43: 491–497.

124. Shi J, Wu Y, Guo S, et al. The efficacy of anti-VEGF antibody-modified liposomes loaded with paeonol in the prevention and treatment of hypertrophic scars. *Drug Dev Ind Pharm* 2019; 45: 439–455.

125. Tavakoli J and Tang Y. Hydrogel based sensors for biomedical applications: an updated review. *Polymers* 2017; 9: 364.

126. Li Y, Wang J, Qian D, et al. Electrospun fibrous sponge via short fiber for mimicking 3D ECM. *Nanobiotechnol* 2021; 19: 131.